JCTC Journal of Chemical Theory and Computation

Article

pubs.acs.org/JCTC

Theoretical Determination of One-Electron Oxidation Potentials for Nucleic Acid Bases

Brian T. Psciuk, Richard L. Lord, Barbara H. Munk, and H. Bernhard Schlegel*

Department of Chemistry, Wayne State University, Detroit, Michigan 48202, United States

Supporting Information

ABSTRACT: The oxidation potentials for N-methyl substituted nucleic acid bases guanine, adenine, cytosine, thymine, uracil, xanthine, and 8-oxoguanine were computed using B3LYP and CBS-QB3 with the SMD solvation model. Acid−base and tautomeric equilibria present in aqueous solution were accounted for by combining standard redox potentials with calculated pK_a and tautomerization energies to produce an ensemble averaged pH dependent potential. Gas phase free energies were computed using B3LYP/aug-cc-pVTZ//B3LYP/6-31+G(d,p) and CBS-QB3. Solvation free energies were computed at the SMD/B3LYP/6-31+G(d,p) level of theory. Compared to experimental results, calculations with the CBS-QB3 level of theory have a mean absolute error (MAE) of ca. 1 kcal/mol for the gas phase proton affinity/gas phase basicity and an MAE of ca. 0.04 eV for the adiabatic/vertical ionization potentials. The B3LYP calculations have a MAE of ∼2 kcal/mol for the proton affinity/gas phase basicity data but systematically underestimated ionization potentials by 0.14−0.21 eV. Solvent cavities for charged solute species were rescaled uniformly by fitting computed pK_a data to experimentally measured pK_a values. After solvent cavity scaling, the MAEs for computed pK_a's compared to experimental results are 0.7 for B3LYP and 0.9 for CBS-QB3. In acetonitrile, the computed $E°(XH^{+\bullet}/XH)$ redox potentials are systematically lower than experimentally measured potentials by 0.21 V for CBS-QB3 and 0.33 V for B3LYP. However, the redox potentials relative to adenine are in very good agreement with experimental results, with MAEs of 0.10 V for CBS-QB3 and 0.07 V for B3LYP. In aqueous solution, B3LYP and CBS-QB3 have MAEs of 0.21 and 0.19 V for $E_7(X^{\bullet},H^{+}/XH)$. Replacing the methyl substituent with ribose changes the calculated E_7 potentials by 0.1−0.2 V. The calculated difference between the guanine and adenine oxidation potentials is too large compared to experimental results, but the calculated difference between guanine and 8-oxoguanine is in good agreement with the measured values.

INTRODUCTION

In biological systems, DNA is persistently exposed to harmful oxidizing agents. Most biological systems possess mechanisms for repairing oxidative damage to DNA. Although these repair mechanisms tend to be highly successful, they cannot repair all damaged DNA. Unrepaired oxidative damage to DNA can lead to mutations that are associated with carcinogenesis, cellular aging, and cellular death.[1−6] Determining the most probable sites for DNA damage is very important for understanding the mechanisms and reaction pathways leading to permanent mutations. It is known that guanine has the lowest oxidation potential among the common nucleobases. There is also a consensus concerning the qualitative trend in oxidation potentials of the common nucleobases.[7] Due to electron transfer processes in DNA, the specific site where oxidative damage takes place may be different from the site of chemical mutation. The electrochemical properties of individual nucleosides are important for the understanding of oxidative damage to DNA. In the present paper, we have used electronic structure calculations and a polarizable continuum solvation model to calculate the electrochemical potentials of some nucleosides.

The one-electron oxidation potentials of nucleosides have been measured by a number of experimental groups in different solvents and at various pH levels in aqueous solution.[8−12] Unfortunately, there is not yet a consensus set of redox potentials for the standard nucleic acids guanine, adenine, cytosine, thymine, and uracil. The various measured values have been discussed extensively, and concerns have been raised such as cyclic voltammetry measurements that involve irreversible redox reactions, solubility issues with specific nucleobases, and inaccurate reference compound potentials.[10,12,13]

The experimental studies by Steenken and co-workers[8,9] and by Seidel et al.[13] have attracted the most attention concerning nucleoside oxidation potentials. The measurements by Steenken and Jovanovic were made in aqueous solution at near physiological pH using chemical oxidation and kinetic rate measurements of reference compounds reacting with the nucleobases. They determined half-cell potentials for guanine at pH 7 (E_7 = 1.29 V) and adenine at pH 3 and pH 5 (E_3 = 1.64 V and E_5 = 1.56 V). Standard potentials ($E°$) were also derived by Steenken and Jovanovic. However, numerous tautomeric and acid−base equilibria control the composition of the reactants and products for redox reactions in aqueous solution. For a redox reaction in aqueous solution at a given pH, the acid dissociation constants (K_a) are needed to relate the measured potentials to $E°$, and the derived $E°$ becomes very sensitive to the K_a values of the oxidized and reduced species. The measurements made by Seidel et al. were performed using cyclic voltammetry in acetonitrile solution. By measuring the one-electron oxidation potentials in an aprotic solvent, they eliminated the complications of acid−base equilibria. However, the cyclic voltammetry measurements were made with a single

Special Issue: Berny Schlegel Festschrift

Received: June 29, 2012
Published: August 29, 2012

voltammetric sweep due to the irreversibility of the redox reactions.

As computational power has increased over the years, sophisticated electronic structure calculations have become practical for larger systems and have provided an alternative way to obtain redox potentials.[14−17] An excellent example of utilizing electronic structure calculations to determine potentials is the recent article by Coote and co-workers benchmarking the absolute reduction potential of the ferrocenium/ferrocene couple in nonaqueous solutions.[15] Thermodynamic cycles similar to the one depicted in Scheme 1 are often used to compute the solution phase free energy difference ($\Delta G_{(sol)}^*$) for a redox reaction. Similar approaches have yielded good results for computing pK_a's.[18,19]

Scheme 1. Thermodynamic Cycle Used in the Calculation of Reduction Potentials

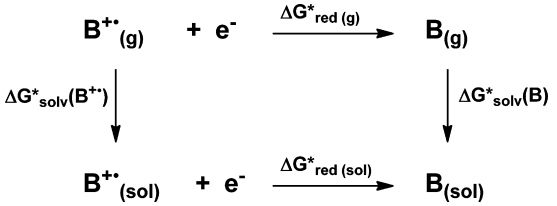

Redox potentials calculated by electronic structure methods are not without issues. The computed solution phase electron attachment or detachment energy for a given species is considered to be an absolute potential, while a potential determined experimentally using electrochemical techniques is measured against a reference electrode and is therefore reported as a relative value. For a calculated absolute potential to be comparable to a measured potential, the absolute potential of the corresponding reference electrode must be subtracted from the calculated absolute potential. The absolute potential of the Standard Hydrogen Electrode (SHE or NHE) has been debated extensively in the literature.[20−23] Deriving an accurate value of E_{SHE}^{obs} requires careful consideration of the proper electron convention, standard state convention, and especially the free energy of a solvated proton.

The present study uses electronic structure calculations to obtain redox potentials and acid dissociation constants that are necessary for calculating pH dependent half-cell potentials for the nucleobases in aqueous solution. Thermodynamic cycles are utilized to obtain reaction free energies for deprotonation reactions and redox processes. Both highly accurate and efficient methods are employed for calculating gas phase free energies. Solvation free energies are estimated using the SMD polarizable continuum model (PCM) by Marenich, Cramer, and Truhlar.[24] Adding explicit solvent molecules can improve the results for PCM calculations in aqueous solution. However this can cause some difficulties in comparing the pK_a's and redox potentials of the nucleobases, since they have differing numbers of hydrogen bonding sites. As an alternative, we calibrate the PCM calculations by adjusting the cavity scaling factors to fit observed pK_a's. The resulting scaling factors will be useful for closely related species, for example, in our next study which focuses on the prediction of pK_a's and redox potentials of transient intermediates in the pathways for oxidative damage to DNA. These data would provide useful information toward a molecular level understanding of why certain DNA oxidation pathways are experimentally observed and others are not.

METHODS

General Description of a Reduction Potential. A standard redox potential is related to the free energy difference of a redox reaction by eq 1

$$E_{red(sol)}^{\circ} = \frac{-\Delta G_{red(sol)}^{*}}{nF} \quad (1)$$

where F is Faraday's constant, $\Delta G_{red(sol)}^*$ is the solution phase standard state free energy change, and n is the number of electrons in the redox process. For all equations shown in the present study, example reactions will be written as one-electron reductions where $n = 1$ throughout. Using the thermodynamic cycle outlined in Scheme 1, $\Delta G_{red(sol)}^*$ is defined in eq 2 for a one-electron reduction of a given radical cation

$$\Delta G_{red(sol)}^{*} = G_{(sol)}^{*}(B) - G_{(sol)}^{*}(B^{+\bullet}) - G_{(g)}^{\circ}(e^{-}) \quad (2)$$

The standard state free energy is expressed in eq 3

$$G_{(sol)}^{*} = (G_{(g)}^{\circ} + \Delta G^{1atm\rightarrow 1M}) + \Delta G_{solv}^{*} \quad (3)$$

where $\Delta G_{(g)}^{\circ}$ is the standard state free energy in the gas phase and ΔG_{solv}^* is the standard state free energy of solvation. $\Delta G^{1atm\rightarrow 1M}$ = 1.89 kcal/mol is the free energy difference for converting from the standard state concentration of 1 atm to the standard state concentration of 1 mol/L. The notation introduced by Ben-Naim and Marcus[25] is used throughout this study, where a degree symbol (°) denotes a standard state of 1 atm and an asterisk (*) denotes 1 mol/L. Substituting eq 3 into eq 2 yields $\Delta G_{red(sol)}^*$

$$\begin{aligned}\Delta G_{red(sol)}^{*} = {} & (G_{(g)}^{\circ}(B) + \Delta G^{1atm\rightarrow 1M} + \Delta G_{solv}^{*}(B)) \\ & - (G_{(g)}^{\circ}(B^{+\bullet}) + G_{(g)}^{\circ}(e^{-}) + \Delta G^{1atm\rightarrow 1M} \\ & + \Delta G_{solv}^{*}(B^{+\bullet}))\end{aligned} \quad (4)$$

and is represented in Scheme 1. A potential calculated using eq 1 yields an absolute potential. Experimental potentials are measured against a reference electrode and are reported as relative half-cell potentials. For comparison with experimental results, we must take the difference of the calculated potential and the absolute potential of the reference electrode. The absolute potential of the standard hydrogen electrode (SHE) in an aqueous solution is estimated to be 4.281 V.[16,17,20,21]

Gas and Solution Phase Calculations. In terms of electronic structure calculations, $G_{(g)}^{\circ}$ is

$$G_{(g)}^{\circ} = E_{el} + ZPE + \Delta G_{0\rightarrow 298K}^{\circ} \quad (5)$$

where E_{el} is the electronic energy (including nuclear repulsion), ZPE is the zero point vibrational energy, and $\Delta G_{0\rightarrow 298K}$ is the calculated thermal free energy change going from 0 to 298 K. In the present study, the gas phase free energy for a given species is obtained by optimizing the structure at the B3LYP level of theory[26−30] with the 6-31+G(d,p) basis set.[31−36] A vibrational frequency calculation is used to determine whether the structure is a minimum or saddle point on the potential energy surface and to compute the ZPE and $\Delta G_{0\rightarrow 298K}$ terms. An additional single point calculation using the aug-cc-pVTZ basis set[37] is used to obtain a more accurate E_{el}. The gas phase free energy at the B3LYP level of theory is given by

$$\begin{aligned}G_{(g)}^{\circ} = {} & E_{el}^{B3LYP/aug\text{-}cc\text{-}pVTZ//B3LYP/6\text{-}31+G(d,p)} \\ & + ZPE^{B3LYP/6\text{-}31+G(d,p)} + \Delta G_{0\rightarrow 298K}^{B3LYP/6\text{-}31+G(d,p)}\end{aligned} \quad (6)$$

An even more accurate method for computing gas phase free energies is the CBS-QB3 compound model chemistry[38,39] which has been shown to predict gas phase thermodynamic properties at near chemical accuracy (MAE of 1.1 kcal/mol).

For a given molecule, Ben-Naim and Marcus[25] described the free energy of solvation (ΔG^*_{solv}) shown in eq 7

$$\Delta G^*_{solv} = G^*_{(sol)}(R') - G^*_{(g)}(R) \tag{7}$$

as the difference between the solution phase free energy of the solution phase optimized molecule, R', and the gas phase free energy of the gas phase optimized molecule, R. The solvation free energy is computed using the SMD implicit solvation model[24] at the B3LYP/6-31+G(d,p) level of theory and includes the electrostatic, cavitation, and dispersion terms. The solution phase free energies are computed by combining the solvation free energies calculated at the B3LYP level of theory with the gas phase free energies calculated with the B3LYP method

$$G^*_{(sol)} = E_{el}^{B3LYP/aug\text{-}cc\text{-}pVTZ//B3LYP/6\text{-}31+G(d,p)} + ZPE^{B3LYP/6\text{-}31+G(d,p)} + \Delta G^{B3LYP/6\text{-}31+G(d,p)}_{0K\rightarrow 298K} + \Delta G^{1atm\rightarrow 1M} + \Delta G^{*SMD/B3LYP/6\text{-}31+G(d,p)}_{solv} \tag{8}$$

and the CBS-QB3 method

$$G^*_{(sol)} = G^{CBS\text{-}QB3}_{(g)} + G^{1atm\rightarrow 1M} + \Delta G^{*SMD/B3LYP/6\text{-}31+G(d,p)}_{solv} \tag{9}$$

All calculations in this study were carried out with a development version of Gaussian.[40] Solution phase calculations were performed using the SMD implicit solvation model.[24] The SMD solvation model uses the integral equation formalism of the polarizable continuum model (IEF-PCM)[41−44] with a parametrized set of atomic radii to calculate the bulk electrostatic energy contribution. The model calculates short-range interaction energies between solvent and solute by using a modified solvent-accessible surface area which incorporates parameters for atomic and molecular surface tensions and hydrogen-bond acidity and basicity. The tessellated solute−solvent boundary uses an average tesserae area of 0.2 Å^2.

The molecules studied here are canonical nucleobases and their derivatives. A nucleic acid base or nucleobase bonded to a ribose or deoxyribose sugar is a nucleoside. Nucleosides bonded to one or more phosphate groups are nucleotides. To compare better with the experimental measurements on nucleosides in solution,[8,9,13] most of the nucleobases calculated in this study have been methylated at the position where the sugar moiety is attached in a nucleoside (for atom numbering see Scheme 2). This avoids complications resulting from protic equilibria and solution phase modeling surrounding the glycosidic nitrogen atoms. The sugar moiety would affect protic equilibria primarily at high pH (>12) where hydroxyl groups of the sugar can be deprotonated. In a previous study investigating reaction pathways following guanine oxidation, replacing the sugar by methyl, hydroxymethyl, and methoxyethyl yielded relative enthalpies that compared well with one another.[45]

Accounting for Multiple Tautomers. The methods discussed above yield redox potentials specific to a given protonation state of the oxidized (Ox_i) and reduced (Red_j) species. During a measurement in aqueous solution, equilibria exist between multiple tautomers (Scheme 3).

Scheme 2. Atomic Numbering for Purines and Pyrimidine Nucleobases[a]

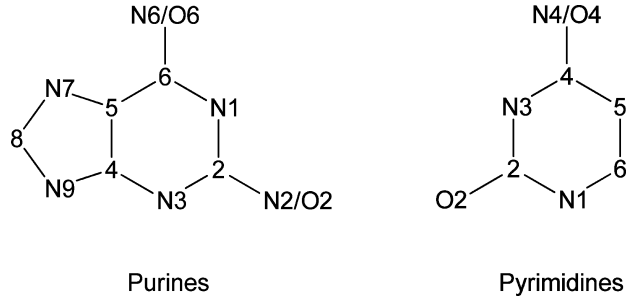

[a]Charge, multiplicity and hydrogen atoms are not explicitly shown.

Scheme 3. Multiple Tautomers Contribute to the Ensemble Reduction Potential

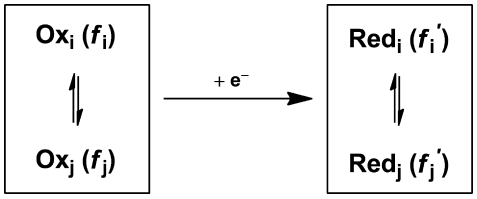

Scheme 4. Thermodynamic Cycle Used in the Calculation of pK_a's

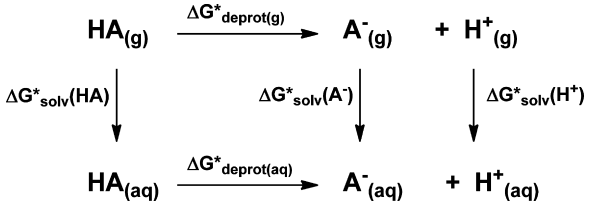

Relative populations of each tautomer are given by a normalized Boltzmann distribution, f, based on the relative free energies of the tautomers

$$f_1 = \frac{[Ox_1]}{[Ox]} = \frac{[Ox_1]}{\sum_n [Ox_n]} = \frac{\exp\left(\frac{-G^*_{1(sol)}}{RT}\right)}{\sum_n \exp\left(\frac{-G^*_{n(sol)}}{RT}\right)} \sum f_n = 1 \tag{10}$$

The tautomer specific equilibrium constant, K^{ij}_{red}, can be related to the ensemble equilibrium constant, K_{red}, using the Boltzmann weighted populations for each species.

$$K^{ij}_{red} = \frac{[Red_j]}{[Ox_i]} = \frac{[Red]f'_j}{[Ox]f_i} = K_{red}\frac{f'_j}{f_i} \tag{11}$$

where f_j' is the population of the jth tautomer of the set of reduced species and f_i is the population of the ith tautomer of the oxidized species. From eq 11, the ensemble equilibrium constant can now be generalized for all possible reductions between tautomers

$$K_{red} = K^{11}_{red}\frac{f_1}{f_1'} = K^{12}_{red}\frac{f_1}{f_2'} = K^{21}_{red}\frac{f_2}{f_1'} = \cdots = K^{ij}_{red}\frac{f_i}{f_j'} \tag{12}$$

The ensemble reduction potential is obtained by inserting the free energy $\Delta G^*_{red(sol)} = -RT\ln(K_{red})$ into the Nernst equation

dx.doi.org/10.1021/ct300550x | J. Chem. Theory Comput. 2012, 8, 5107−5123

Table 1. Experimental and Calculated Gas Phase Basicities and Proton Affinities for Nucleic Acid Bases in kcal/mol

$A + H^+ \rightarrow AH^+$						
	H^+ site	exptl.[a]	CBS-QB3	G3B3	B3LYP[c]	B3LYP[d]
proton affinity						
guanine	N7	229.3	227.6[b]	228.2[b]	230.8	230.5[b]
adenine	N1	225.3	223.6[b]	224.9[b]	227.1	226.7[b]
cytosine	N3	227.0	226.9[b]	227.6[b]	229.2	228.9[b]
1-methyl cytosine	N3	230[e]	230.1[c]	230.9[c]	232.7	232.4[c]
thymine	O4	210.5	209.6[c]	210.6[c]	211.1	210.8[c]
uracil	O4	208.6	206.8[c]	207.7[c]	208.2	207.8[c]
MAE to exptl.			*1.1*	*0.7*	*1.5*	*1.3*
gas phase basicity						
guanine	N7	221.7	220.2[b]	220.9[b]	223.3	223.0[b]
adenine	N1	218.1	216.3[b]	217.1[b]	218.9	218.3[b]
cytosine	N3	219.0	218.9[b]	219.8[b]	221.0	219.9[b]
1-methyl cytosine	N3	223[e]	222.4[c]	223.3[c]	224.8	224.5[c]
thymine	O4	203.2	201.7[c]	202.6[c]	203.2	202.8[c]
uracil	O4	201.2	198.9[c]	199.8[c]	200.2	199.9[c]
MAE to exptl.			*1.3*	*0.8*	*1.2*	*0.9*
$A^- + H^+ \rightarrow AH$						
	H^+ site	exptl.[e]	CBS-QB3	G3B3	B3LYP[c]	B3LYP[d]
proton affinity						
guanine	N1		337.7[b]	338.2[b]	340.1	339.9[b]
guanine	N9	335	335.2[c]	335.9[c]	338.1	337.8[c]
adenine	N9	335	335.3[c]	335.9[c]	338.5	338.2[c]
cytosine	N1	342	344.8[c]	345.3[c]	347.1	346.8[c]
thymine	N3	346	346.3[b]	347.0[b]	347.1	346.9[b]
thymine	N1	335	335.4[c]	336.2[c]	335.9	336.6[c]
uracil	N3	347	346.3[b]	347.0[b]	346.6	346.9[b]
MAE to exptl.			*0.8*	*1.2*	*2.4*	*2.2*
gas phase basicity						
guanine	N1		330.2[b]	330.6[b]	332.6	332.3[b]
guanine	N9	328	327.7[c]	328.4[c]	330.6	330.3[c]
adenine	N9	329	328.8[c]	328.7[c]	331.7	331.4[c]
cytosine	N1	335	337.5[c]	337.8[c]	339.9	339.7[c]
thymine	N3	339	338.5[b]	339.1[b]	339.3	339.0[b]
thymine	N1	328	327.9[c]	328.7[c]	328.4	329.1[c]
uracil	N3		338.1[b]	338.6[b]	338.7	338.4[b]
MAE to exptl.			*0.7*	*0.9*	*2.2*	*2.1*

[a]Refs 78−81. experimental error of ±2 kcal/mol. [b]Ref 54. [c]Present study. [d]Calculated using the B3LYP/6-311++(3df,2p)//B3LYP/6-31++G(d,p) level of theory.[54] [e]Experimental error of ±3 kcal/mol.[56,82,83]

$$E^{\circ}_{\mathrm{red(sol)}} = \frac{RT}{F}\ln(K_{\mathrm{red}}) \tag{13}$$

Substituting eq 12 into eq 13 yields the ensemble reduction potential expressed in terms of tautomer specific potentials

$$E^{\circ}_{\mathrm{red(sol)}} = {E^{\circ}_{\mathrm{red(sol)}}}^{ij} + \frac{RT}{F}\ln(f_i) - \frac{RT}{F}\ln(f_j') \tag{14}$$

Calculating pK_a and E_7. Experimental standard redox potentials are usually derived from potentials measured at a specific pH in aqueous solutions using the Nernst half-cell equation shown in eq 15

$$E_{1/2} = E^{\circ} - \frac{RT}{F}\ln\left(\frac{[\mathrm{Red}]}{[\mathrm{Ox}]}\right) \tag{15}$$

Table 2. Experimental and Calculated Gas Phase Adiabatic (AIE) and Vertical Ionization Energies (VIE) for Nucleic Acid Bases (in eV)

adiabatic						
	exptl.[a,b]	CBS-QB3	G3-B3	B3LYP[c]	BP86[c]	PMP2[d]
guanine	7.77	7.85	7.88	7.66	7.65	7.90
adenine	8.26	8.28	8.30	8.07	8.04	8.23
cytosine	8.68	8.71	8.83	8.56	8.50	8.78
thymine	8.87	8.91	8.93	8.72	8.64	8.74
uracil	9.32	9.32	9.35	9.21	9.14	9.36
MAE to exptl.[e]		*0.03*	*0.08*	*0.14*	*0.19*	*0.08*
		CBS-QB3		B3LYP[c]		
9-methylguanine		7.65		7.47		
9-methyladenine		8.10		7.89		
1-methylcytosine		8.35		8.27		
1-methylthymine		8.54		8.38		
1-methyluracil		8.92		8.81		
				B3LYP[c]		
guanosine				7.24		
adenosine				7.84		
cytidine				8.05		
thymidine				7.96		
uridine				8.28		
vertical						
	exptl.	CBS-QB3	G3-B3	B3LYP[j]	BP86[j]	PMP2[d]
guanine	8.28[e]	8.33	8.29	8.10	8.41	8.33
adenine	8.48[f]	8.51	8.47	8.25	8.21	8.62
cytosine	8.89[g]	8.86	8.91	8.69	8.64	8.69
thymine	9.20[h]	9.18	9.21	9.00	8.88	9.07
uracil	9.59[i]	9.58	9.56	9.45	9.29	9.43
MAE to exptl.		*0.03*	*0.02*	*0.18*	*0.23*	*0.13*
	exptl.	CBS-QB3	G3-B3	B3LYP[j]	BP86[j]	PMP2
9-methylguanine	8.02[e]	8.03	8.08	7.81	7.76	8.17
9-methyladenine	8.39[f]	8.37	8.30	8.09	8.03	8.45
1-methylcytosine	8.65[g]	8.54	8.70	8.43	8.36	8.49
1-methylthymine	8.79	8.83	8.85	8.64	8.52	8.69
1-methyluracil	9.2	9.15	9.21	9.04	8.93	9.01
MAE to exptl.		*0.05*	*0.05*	*0.21*	*0.29*	*0.13*

[a]Ref 84. Estimated accuracy of ±0.05 V. [b]A separate set of values is given by NIST: guanine, 7.85 eV; adenine, 8.3 ± 0.1 eV; cytosine, 8.45 eV; thymine, 9.0 ± 0.1 eV; uracil, 9.2 ± 0.1 eV.[78] [c]For the given level of theory, the calculated AIE is the difference in energy between the radical cation and neutral species where the energy of each species is the sum of the $\Delta G_{0\rightarrow 298K}$ correction using the 6-31+G(d,p) basis set and E_{0K} using the aug-cc-pVTZ basis set on the geometry optimized at the 6-31+G(d,p) basis set. [d]Crespo-Hernandez et al. study calculated at PMP2/6-31++G(d,p) level of theory where adiabatic energies are for ZPE at HF/6-31++G(d,p) level of theory.[60] [e]Ref 62. [f]Ref 63. [g]Ref 64. [h]Ref 65. [i]Ref 66. [j]For the given level of theory, the calculated VIE is the difference in E_{0K} using the aug-cc-pVTZ basis set between the radical cation and neutral species at the geometry of the neutral species optimized using the 6-31+G(d,p) basis set.

Conversely, a pH dependent potential can be derived from a calculated standard redox potential using the equilibrium concentrations of the reduced and oxidized species. In protic solvents, the concentrations of alternate protonation states existing in solution within the applicable pH range need to be included for both the reduced and oxidized species. Assuming dilute concentrations (low ionic strength), a functional form can be derived[46,47] for calculating the pH dependent potentials

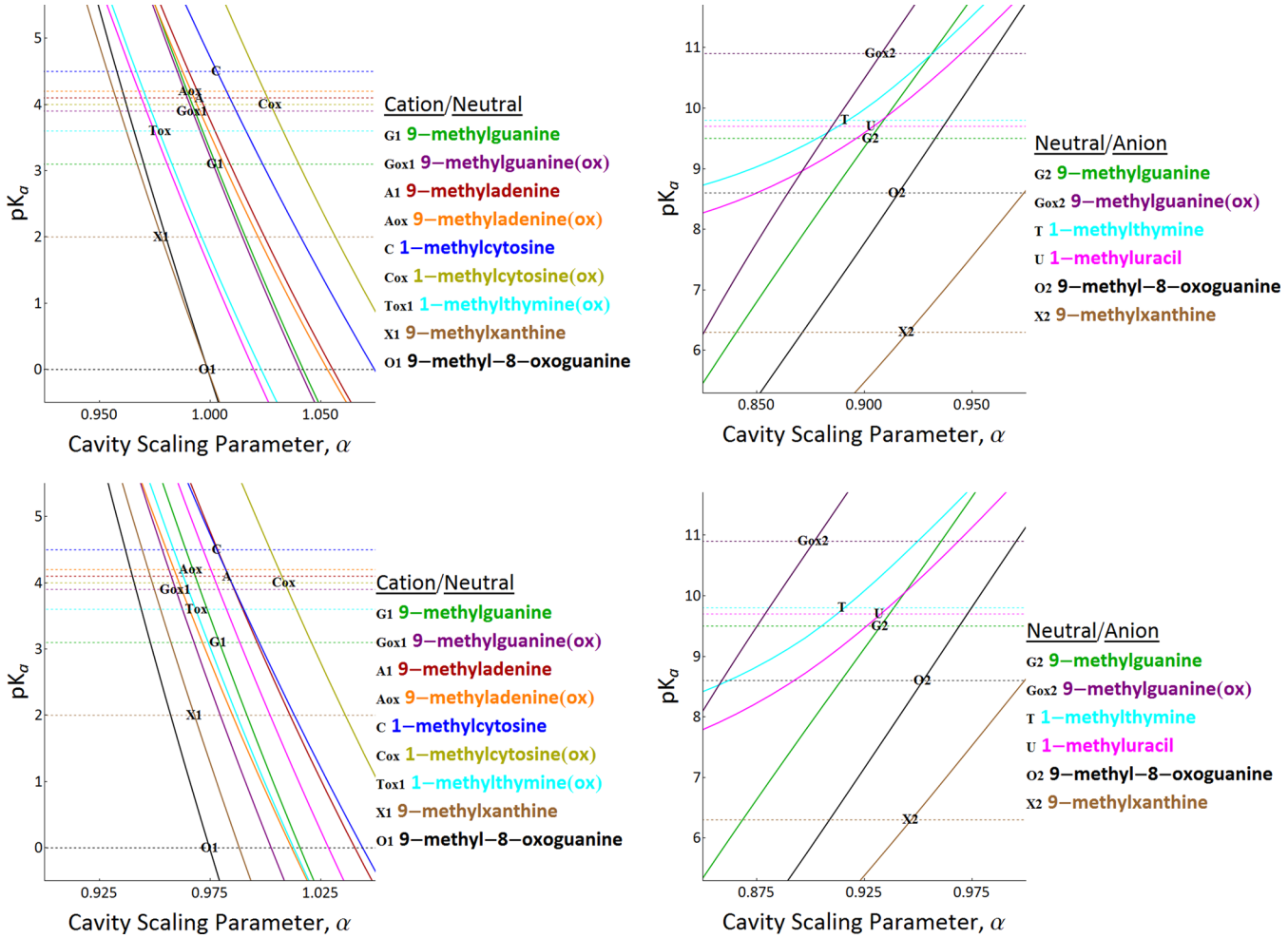

Figure 1. Effect of changing the solvent cavity parameter on the calculated pK_a for the B3LYP and CBS-QB3 methodologies. Each solid curve represents a third order polynomial fit of calculated pK_a data points collected at scaled solvent cavities. For all neutral species shown, the solvent cavity was left unscaled (α = 1.0), while the solvent cavity scaling values for ionic species were varied. Horizontal dotted lines represent experimentally measured pK_a's. The intersection of a calculated pK_a curve with an experimental pK_a (depicted by a symbol specific to the nucleobase) indicates the optimal solvent cavity scaling value for a given nucleobase. The optimal solvent cavity scaling parameters for B3LYP are 0.9, 1.0, and 1.0 for anionic, cationic, and neutral species, respectively. The optimal scaling factors for CBS-QB3 are 0.925, 0.975, and 1.0 for anionic, cationic, and neutral species, respectively.

for a nucleobase that has three K_a's for the reduced form and two K_a's for the oxidized form

$$E_{pH} = E^{\circ}(X^{\bullet}, H^{+}/XH) + \frac{RT}{F}\ln\left(\frac{K_{a1o}}{K_{a1r}}\right) + \frac{RT}{F}\ln\left(\frac{K_{a1r}K_{a2r}K_{a3r} + K_{a1r}K_{a2r}10^{-pH} + K_{a1r}10^{-2pH} + 10^{-3pH}}{K_{a1o}K_{a2o} + K_{a1o}10^{-pH} + 10^{-2pH}}\right) \quad (16)$$

Similar expressions can be obtained for cases with different numbers of K_a's, e.g.

$$E_{pH} = E^{\circ}(X^{\bullet}, H^{+}/XH) + \frac{RT}{F}\ln\left(\frac{K_{a1o}}{K_{a1r}}\right) + \frac{RT}{F}\ln\left(\frac{K_{a1r}K_{a2r} + K_{a1r}10^{-pH} + 10^{-2pH}}{K_{a1o} + 10^{-pH}}\right) \quad (17)$$

"XH" signifies a specific nucleic acid species in the reduced or closed shell neutral state, and "X$^{\bullet}$" is the corresponding oxidized species that has been deprotonated following the one-electron transfer comprising the predicted redox couple for processes occurring in aqueous solution at pH 7. "o" stands for the oxidized species K_a, and "r" stands for the reduced species K_a. For a redox potential in aqueous solution, acid dissociation constants of the oxidized species (K_{ao}) and reduced species (K_{ar}) account for the concentrations of the relevant protonation states. For example, the experimental values needed for the pH dependent potential of guanosine are pK_{a1r} = 1.9, pK_{a2r} = 9.3, pK_{a3r} = 12.5, pK_{a1o} = 3.9, pK_{a2o} = 10.9, and E° = 1.58 V.[9,48] Further discussions regarding the pH dependence of reduction potentials can be found in the literature.[46,47]

Acid dissociation constants for short-lived radical species may be difficult to measure experimentally, and very few measured pK_a's are available for radical nucleobase species. Additionally, discrepancies between experimentally measured pK_a's of closed shell species are often larger than the reported measurement error. Therefore, we have decided to also calculate the pK_a's needed for pH dependent potentials. Previous computational studies by Verdolino et al.[49] and Jang et al.[50,51] have calculated tautomer specific and ensemble pK_a's for standard and modified nucleic acid bases using a protocol very similar to the one described here. To be consistent, we use calculated pK_a's to

Table 3. Experimental and Calculated pK_a Values

	exptl.		CBS-QB3	B3LYP	B3LYP[j]	other calcd.
	methyl subst.	ribose subst.	methyl subst.	methyl subst.	ribose subst.	unsubst.
			guanine			
pKa1	3.1[a]	1.9[d]	3.50	3.20	1.47	3.4,[k] 3.15[m]
pKa2	9.5[a]	9.2[d]	9.10	9.36		9.6,[k] 9.60[m]
$pKa1_{ox}$		3.9[e]	2.53	3.34	2.61	4.01[l]
$pKa2_{ox}$		10.9[e]	11.88	10.32		
			adenine			
pKa1	4.1[b]	3.6[f]	4.89	3.79	4.43	4.2[k]
pKa_{ox}		4.2[g]	2.82	3.90	3.18	2.01[l]
			cytosine			
pKa1	4.5	4.2[f]	4.80	4.71	4.54	4.2[k]
pK_{aox}		~4[e]	6.72	5.69	6.46	3.37[l]
			thymine			
pK_a		9.8[f]	9.96	9.98		10.5[k]
pK_{aox}		3.6[e]	3.04	1.69	2.88	6.40[l]
			uracil			
pK_a	9.7	9.2[f]	9.33	9.59		
pK_{aox}			4.06	1.52	1.61	
			xanthine			
pKa1	2.0[c]	1.1[c]	1.31	0.44	−1.46	
pKa2	6.3[c]	5.7[c]	5.29	4.76		
$pKa1_{ox}$			−4.03	−5.52	−5.98	
$pKa2_{ox}$			7.54	6.98		
			8-oxoguanine			
pKa1		0.1[h]	−0.04	−0.12	−1.96	0.22[m]
pKa2		8.6[h]	7.09	8.13		8.0[k], 8.69[m]
$pKa1_{ox}$			0.06	−0.28	−0.54	6.83[l]
$pKa2_{ox}$		6.6[i]	4.83	5.50		
MAE to exptl.			*0.88*	*0.66*	*1.31*	

[a]Ref 85. [b]Ref 86. [c]Ref 87. [d]Ref 88. [e]Ref 11. [f]Ref 48. [g]Value is for deoxyribose substituted species.[89] [h]Ref 90. [i]Ref 8. [j]Computed using B3LYP gas phase free energies for nucleosides. Solvent cavities were not scaled for calculations involving nucleosides. [k]Verdolino et al. calculated ensemble pK_a's for nonmethylated nucleobases using Boltzmann-weighting for alternate tautomers at the B3LYP level of theory.[49] [l]Baik et al. calculated tautomer specific pK_a's for nucleobases at PW91 level of theory.[59] [m]Goddard and co-workers calculated ensemble pK_a's for nonmethylated nucleobases using Boltzmann-weighting for alternate tautomers at the B3LYP level of theory.[50,51]

obtain the pH dependence of the calculated redox potentials. The ensemble pK_a tautomers can be assigned Boltzmann weighted populations

$$pK_a = pK_a^{ij} - \log(f_i) + \log(f_j') \quad (18)$$

where f_j' is the population of the jth tautomer of the set of deprotonated species and f_i is the population of the corresponding ith tautomer of the protonated species. The tautomer specific pK_a is

$$pK_a^{ij} = \frac{\Delta G^{*ij}_{deprot(aq)}}{2.303RT} \quad (19)$$

and $\Delta G^*_{deprot(aq)}$ is calculated using the thermodynamic cycle in Scheme 4.

The aqueous free energy for the deprotonation reaction is given by

$$\Delta G^*_{deprot(aq)} = G^\circ_{(g)}(A^-) + \Delta G^*_{solv}(A^-) + G^\circ_{(g)}(H^+) + \Delta G^*_{solv}(H^+) - G^\circ_{(g)}(HA) - \Delta G^*_{solv}(HA) + \Delta G^{1atm\rightarrow 1M} \quad (20)$$

In this study, the literature value $\Delta G^*_{solv}(H^+) = -265.9$ kcal/mol[22] is used for the aqueous solvation free energy of H^+.

The gas phase energies for the proton and the electron at 0 K are zero. The gas phase free energy for H^+ at 298 K is $\Delta G^\circ_{(g)}(H^+) = -6.287$ kcal/mol and is derived from $G^\circ_{(g)} = H^\circ_{(g)} - T{\cdot}S^\circ_{(g)}$ where $E_{0K} = 0$ au, $H^\circ_{(g)} = 5/2RT = 1.48$ kcal/mol, and $S^\circ_{(g)} = 26.05$ cal/mol·K. Similarly, the gas phase free energy of the electron at 298 K is $G^\circ_{(g)} = -0.867$ kcal/mol using $H^\circ_{(g)} = 0.752$ kcal/mol and $S^\circ_{(g)} = 5.434$ cal/mol·K based on Fermi-Dirac statistics.[52,53]

RESULTS AND DISCUSSION

Redox potentials in solution include the intrinsic energy of adding or removing an electron along with the solvation energy of the oxidized and reduced species. For the nucleobases considered here, these are neutral, cationic, and anionic species depending on the experimental pH conditions and whether or not a proton transfer accompanies the electron transfer. To compare with experimentally observed values, the relative abundance of the various tautomers at each redox level must be taken into account. In aqueous solution, acid−base equilibria must also be included in the treatment. To assess the accuracy of the various levels of theory, we first compared the calculated ionization potential and gas phase basicity with experimental values. Then, we examined the suitability of the SMD solvation model by calculating the pK_a's for the nucleobases. To obtain ensemble averaged pK_a's, tautomeric equilibria are included for

the different protonation states. Solvent cavity scaling parameters are adjusted to improve the agreement with experimental results. Next, redox potentials are calculated in acetonitrile, where acid–base equilibria are absent. Finally, redox potentials are calculated in aqueous solution as a function of the pH, taking into account both the tautomeric and acid–base equilibria.

Gas Phase Energies. For the gas phase reaction $A + H^+ \rightarrow AH^+$ (the upper part of Scheme 4), the proton affinity (PA) is the reaction enthalpy and the gas phase basicity (GB) is the reaction free energy. Table 1 compares computed and measured PA and GB energies for unsubstituted nucleobases and their anions. The results from a theoretical study by Moser et al.[54] are also listed for comparison. The CBS-QB3[38,39] and the G3B3[55] compound model chemistries are the most accurate calculations in the table. Compared to experimental results, the mean absolute errors (MAE) for CBS-QB3 and G3B3 are 0.7–1.3 kcal/mol and are well within the estimated experimental error of 2–3 kcal/mol. Both York and co-workers[54] and Lee and co-workers[56] noted that their calculated values for proton affinities of neutral thymine and uracil disagreed with experimental results by as much as 4 kcal/mol. Calculations by Wolken and Turecek[57] showed that the most stable protonated isomer of uracil is the N-1 deprotonated 2,4-dihydroxy form, rather than the expected N-1 protonated 2-oxo,4-hydroxy form (Scheme 5). The present B3LYP, G3B3, and CBS-QB3 calculations confirm that the N-1 deprotonated 2,4-dihydroxy form is the most stable isomer for both thymine and uracil. The PA and GB for the neutrals and anions calculated with B3LYP/aug-cc-pVTZ are on average 1.7 and 2.1 kcal/mol higher than the experimental and CBS-QB3 values, respectively.

Scheme 5. Lowest Energy Gas Phase Tautomers of Protonated Uracil/Thymine

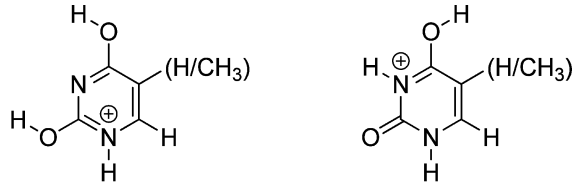

N-1 deprotonated 2,4-dihydroxy | N-1 protonated 2-oxo-4-hydroxy

Table 2 compares the calculated vertical and adiabatic ionization energies with experimental values. The adiabatic ionization energy is the gas phase analogue of the one-electron oxidation potentials we are interested in, and systematic errors in the ionization energies should be reflected in the redox potentials. The best agreement with experimental results is found for CBS-QB3 (MAE = 0.03–0.05 eV) and G3B3 (MAE = 0.05–0.08 eV). The MAEs are comparable to the estimated experimental error of ±0.05 eV. The B3LYP/aug-cc-pVTZ values are systematically too low when compared to experimental results (MAE = 0.14–0.21 eV) and CBS-QB3 (MAE = 0.17–0.19 eV). The BP86/aug-cc-pVTZ calculations yield a slightly larger underestimation than B3LYP (MAE 0.19–0.29 eV vs experiment). This underestimation of ionization energies is known to be characteristic of the B3LYP and other DFT levels of theory as other studies have shown.[54,58,59] The ionization energies calculated by Crespo-Hernandez et al.[60] at the PMP2 level of theory[61] with a 6-31++G(d,p) basis have smaller MAEs than the DFT results, but the deviations are less systematic.

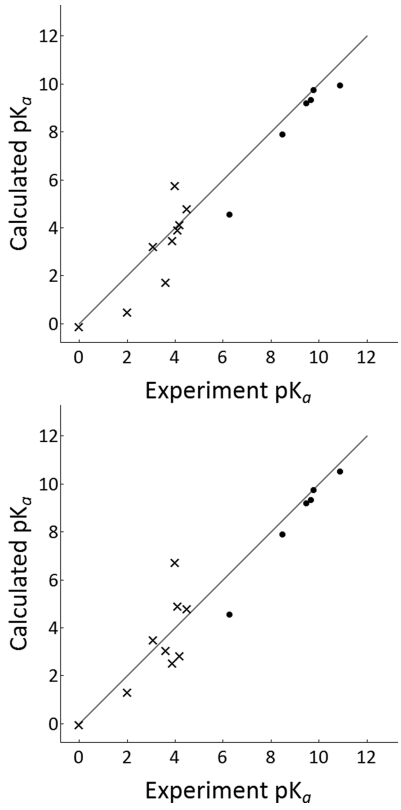

Figure 2. Linear correlation plots of calculated pK_a's versus experimental pK_a's. Cation deprotonations are signified by a cross, and neutral deprotonations are signified by a dot.

Experimental data show that methyl substitution of the nucleobases lowers the vertical ionization energy by 0.26 eV for 9-methylguanine,[62] 0.09 eV for 9-methyladenine,[63] 0.24 eV for 1-methylcytosine,[64] 0.40 eV for 1-methylthymine,[65] and 0.39 eV for 1-methyluracil.[66] The calculated methyl substitution effects on the vertical ionization energy are in good agreement with experimental results (MAE = 0.05 eV for CBS-QB3 and G3B3). Although there are no experimental data, calculations show that replacing the methyl substituent with ribose lowers the ionization energy by an additional 0.1–0.4 eV. Calculations by Crespo-Hernandez et al.[67] find similar effects for methyl and 2′-deoxyribose substitution of the bases. As recommended by Crespo-Hernandez et al., the present calculations use the *anti* orientation for the nucleosides since this conformation is more relevant for the geometries in solution and in DNA.

Solvent Scaling Parameters. Calculated solvation free energies for ionic species generally have larger errors than for neutral species. A relatively simple way of addressing this error is either to scale the individual atomic radii used to create the solvent cavity or scale the entire solvent cavity. In addition to compensating for different errors in solvation free energies for charged species and for specific hydrogen bonding between solvent and solute, this may also adjust for systematic errors in the calculated gas phase free energies of the molecular species. Other studies have incorporated cavity scaling techniques with success.[14,49,68–72] Figure 1 shows the pK_a's as a function of the cavity scaling parameter α for the cations and the anions (the solvent cavities for the neutrals were left unscaled, α = 1.00). The scale factors were chosen by comparison with experimental results, minimizing the average error and rounding to the nearest 0.025. The optimal scale factors at the CBS-QB3 level

dx.doi.org/10.1021/ct300550x | J. Chem. Theory Comput. 2012, 8, 5107–5123

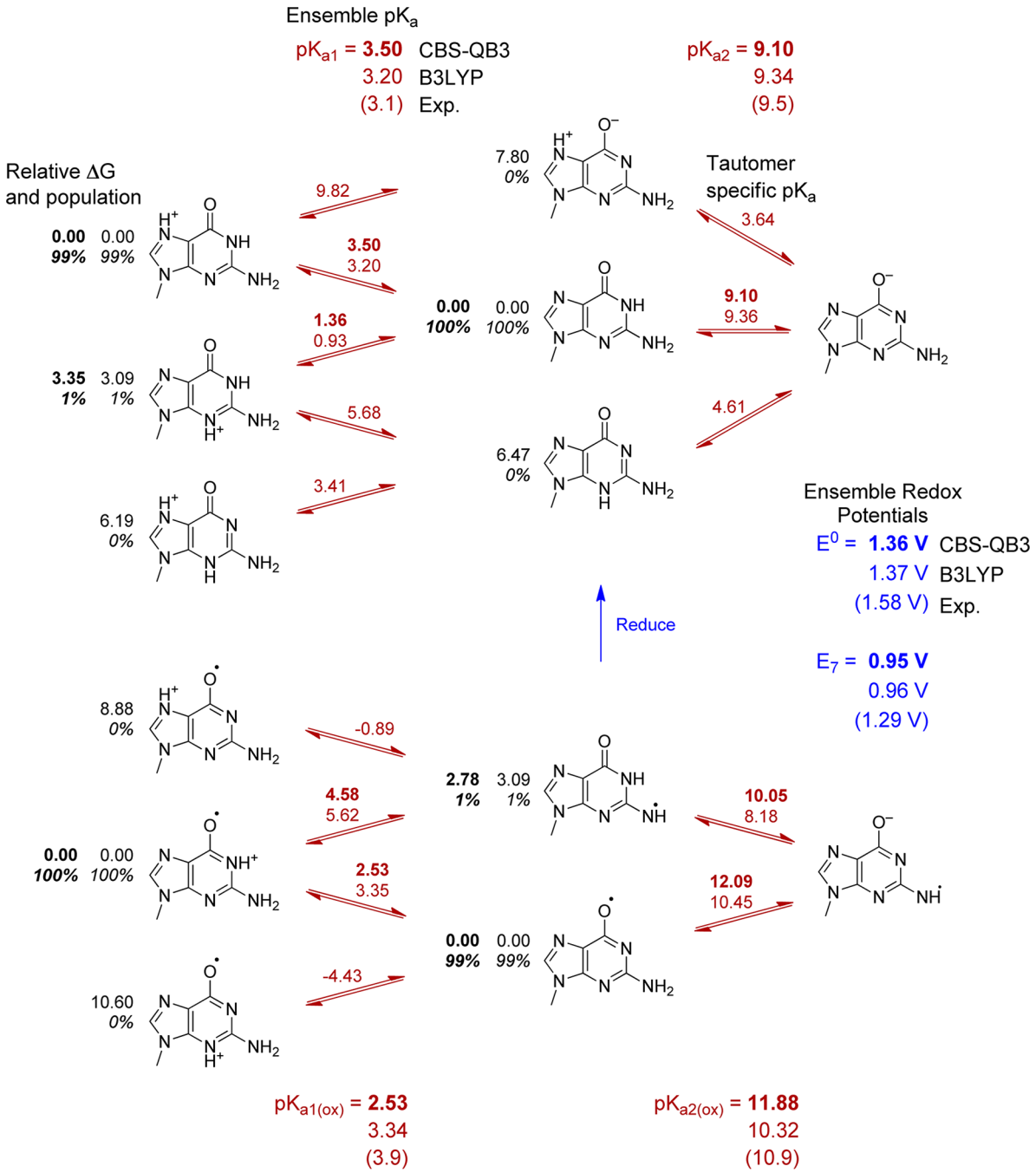

Figure 3. Calculated pK_a's and oxidation potentials for 9-methylguanine. Experimentally measured values are shown in parentheses. CBS-QB3 calculated values are shown in bold face text, while B3LYP calculated values are shown in regular text. Black numbers to the left of each isomer indicate the relative free energy in kcal/mol (regular font) and the population in percentage (italics). Red numbers shown in between isomers indicate calculated pK_a's for the specific isomers, while red numbers on the top and bottom of the figure indicate the ensemble averaged pK_a for each acid/base equilibrium. Blue numbers shown between the reduced (top) and oxidized species (bottom) indicate calculated one-electron oxidation potentials E° and E_7.

of theory were found to be $\alpha = 0.975$ for the cations and $\alpha = 0.925$ for the anions. The corresponding values for the B3LYP calculations are $\alpha = 1.00$ for the cations and $\alpha = 0.90$ for the anions. A previous study by Verdolino et al.[49] found $\alpha = 0.91$ for the cations and $\alpha = 0.83$ for the anions for B3LYP calculations on a smaller set of comparisons for unoxidized nucleobases. Their study used an earlier version of the IEF-PCM solvation model with UFF atomic radii and a solvent excluding surface. The fact that the present scale factors are closer to unity reflects improvements in the solvation model.

Calculated pK_a Values. Table 3 summarizes the pK_a's calculated for the methyl substituted nucleobases at the CBS-QB3 and B3LYP levels of theory with the optimal solvent cavity scaling factors. These values are compared with calculations by Baik et al.[59] and Verdolino et al.[49] Some pK_a's have been measured for the methyl substituted bases, but more experimental data are available for the nucleosides (sugar substituted nucleobases). Where available, the experimental value for the methyl substituted base is used for comparison with the calculations. The difference between the experimental pK_a's for the methyl- and

dx.doi.org/10.1021/ct300550x | J. Chem. Theory Comput. 2012, 8, 5107−5123

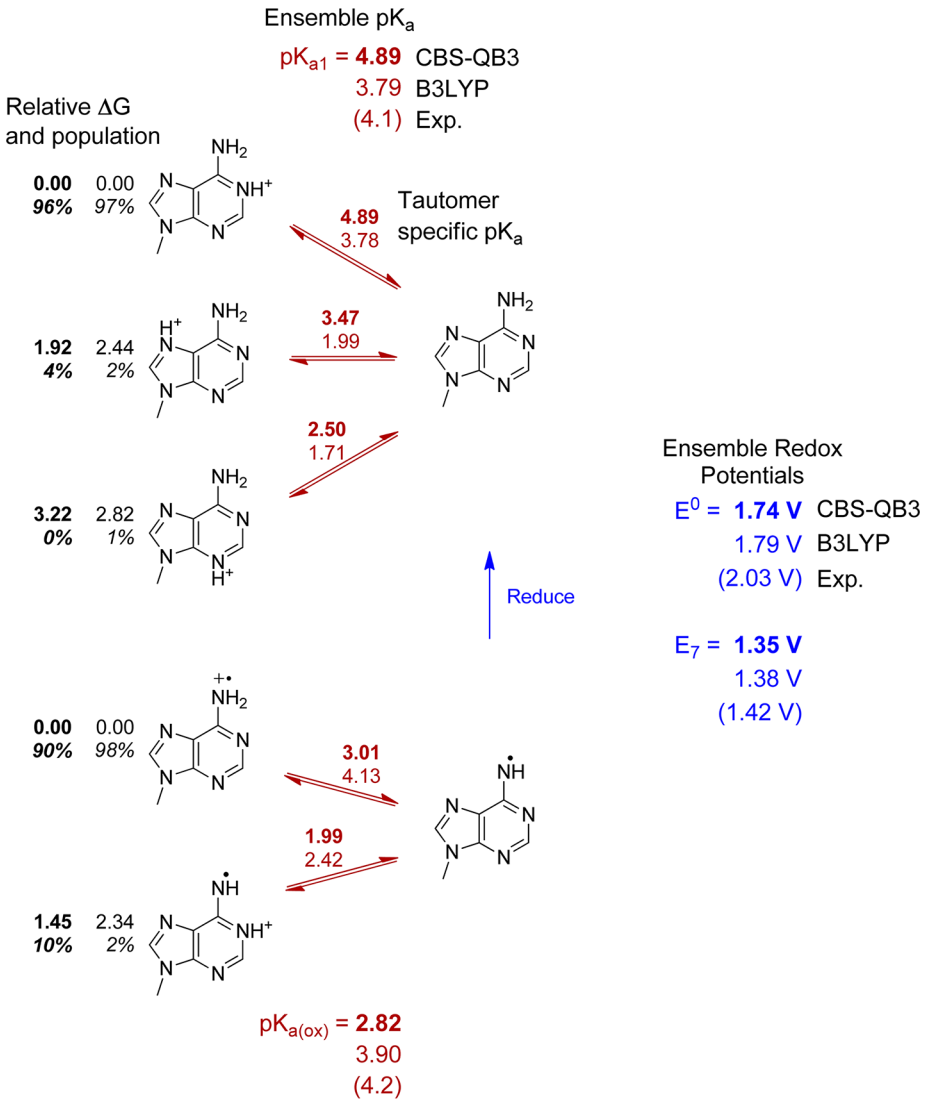

Figure 4. Calculated pK_a's and oxidation potentials for 9-methyladenine. See Figure 3 caption for details.

sugar-substituted bases is usually less than 1 pK_a unit. Deprotonation of the sugar occurs at pH ~ 12.5 and above; therefore, pK_a values greater than 12 are not included in the comparisons. Figure 2 compares the experimental and calculated pK_a's. The MAE is 0.9 for CBS-QB3 and 0.7 for B3LYP. The SMD method has an MAE of ca. 1 kcal/mol for the solvation free energy of neutral molecules and an MAE of ca. 4 kcal/mol for singly charged ionic molecules, translating to an MAE of roughly 3 pK_a units. The good MAE values achieved in the computed pK_a's can be attributed in part to the solvent cavity scaling.

For the unoxidized bases, the present calculations agree quite well with the results obtained by Verdolino et al. and with calculations by Goddard and co-workers[50,51] on guanine and 8-oxoguanine. For the oxidized bases, there is a larger spread in values between the present CBS-QB3 and B3LYP calculations and the PW91 calculations of Baik et al. Comparison with other calculations in the literature are hampered by the fact that they rely on linear regressions rather than direct calculations of the pK_a's. The pK_a's for deprotonation of the cations are typically less than 6, while the pK_a's for deprotonation of the neutrals are higher than 7 (9-methylxanthine is an exception). Consequently, oxidation of a neutral base makes it much more acidic, and oxidation at pH 7 will typically be accompanied by loss of a proton.

The calculated pK_a's listed in Table 3 are ensemble averages. The tautomer specific pK_a's and relative energies of the tautomers are shown in Figures 3−9. In most cases, one tautomer dominates in solution (the anion of 9-methyl-8-oxoguanine is an exception). In almost all cases, the most stable tautomer of the oxidized and unoxidized species is the same, even though the relative energies of their higher lying tautomers differ. For 9-methylguanine, adenine, xanthine, and their oxidized forms, protonation occurs at N7, but for 9-methyl-8-oxoguanine, protonation occurs at N1. Deprotonation of N1 is preferred for neutral and oxidized 9-methylxanthine and oxidized 9-methyl-8-oxoguanine, but deprotonation of N3 and N7 are nearly equal in energy for 9-methyl-8-oxoguanine. For most of the remaining structures, protonation or deprotonation occurs at a ring nitrogen in preference to an $-NH_2$ group. Deprotonation of an exocyclic $-NH_2$ to form $-NH^-$ is strongly disfavored for the neutral species, but deprotonation of $-NH_2^+$ is more facile in the corresponding oxidized species (e.g., pK_{a2r} versus pK_{ao} of 9-methyladenine and 1-methylcytosine). The enol tautomers of the oxidized species are 5−15 kcal/mol higher in energy than the keto forms.

dx.doi.org/10.1021/ct300550x | J. Chem. Theory Comput. 2012, 8, 5107−5123

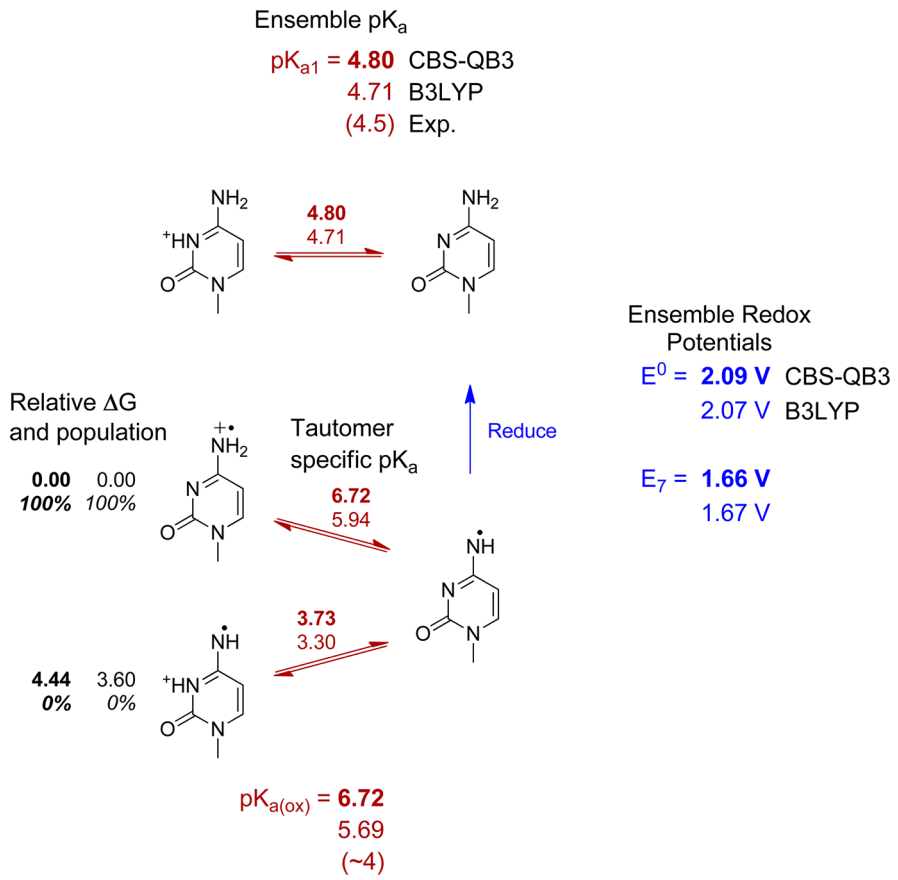

Figure 5. Calculated pK_a's and oxidation potentials for 1-methylcytosine. See Figure 3 caption for details.

Redox Potentials in Acetonitrile. Redox potentials in acetonitrile should be easier to compute than in aqueous solution because they are not complicated by acid–base equilibria, and the SMD solvation model should be well suited for aprotic solvents. The $E°(XH^{+\bullet}/XH)$ redox potentials for the nucleobases listed in Table 4 were calculated without cavity scaling. To check the accuracy of the present approach, standard reduction potentials were calculated for a few compounds with well-established values (4-methyl aniline, anisole, and naphthalene). The MAE in the calculated reduction potentials is 0.02 V for CBS-QB3 and 0.25 V for B3LYP and is similar to the MAEs for their gas phase ionization potentials. For a much larger set of quinones and azacyclic compounds in aprotic solvents, Leszczynski and co-workers find MAEs in the range of 0.09–0.21 V, depending on the combination of density functional, basis set, and solvation model.[14] For a diverse set of 270 organic molecules, Fu et al.[70] found that B3LYP/6-311++G(2df,2p) underestimated the ionization potential by 0.28 eV. Using PCM solvation with Bondi radii scaled by 1.20, and correcting the ionization potentials by 0.28 V, Fu et al. found a standard deviation of 0.17 V for the reduction potentials in acetonitrile. These data suggest that the inherent uncertainty in the calculated redox potentials in acetonitrile may be 0.1–0.2 V even after systematic errors are taken into account.

Table 4 compares the computed redox potentials in acetonitrile with the experimental values for the nucleosides in acetonitrile solution measured versus SCE by Seidel et al.[13] The calculated values for the methyl substituted nucleobases are on average 0.21 and 0.33 V too low for CBS-QB3 and B3LYP, while the values for nucleosides are 0.28 V too low for B3LYP. These deviations are somewhat larger than the MAEs for the corresponding ionization potentials in Table 2. The effect of the systematic errors in the ionization potentials and the solvation energies can be reduced significantly by comparing the relative values of redox potentials as shown in lower half of Table 4. Using adenine as a reference, the calculated relative redox potentials are in much better agreement with experimental values (MAE = 0.10 V for CBS-QB3 and 0.07 V for B3LYP) and with each other (MAE = 0.04 V). Both the CBS-QB3 and B3LYP calculations yield a redox potential for 9-methylguanine that is 0.4–0.5 V lower than 9-methyladenine in agreement with Seidel et al. The calculations find the redox potentials of 1-methylcytidine, 1-methylthymine, and 9-methylxanthine are similar to 9-methyladenine, while 1-methyluracil is 0.3–0.4 V higher and 9-methyl-8-oxoguanine is 0.8 V lower. Replacing the methyl substituent with ribose increases the redox potentials relative to adenine by approximately 0.10 V.

Redox Potentials in Water. The determination of redox potentials of the nucleobases in aqueous solution is considerably more difficult than in acetonitrile. Experimental measurements are hampered by problems due to solubility and irreversibility. Calculations are complicated by acid–base equilibria and hydrogen bonding in aqueous solution. To help separate the effects of solvation from acid–base equilibria, we first compare the $E°(XH^{+\bullet}/XH)$ redox potentials in water (Table 5) with the corresponding values in acetonitrile (Table 4). The calculated redox potentials of the nucleobases relative to adenine in water compare well with the results measured by Seidel et al. in acetonitrile (MAE = 0.13 V).[13] The relative values of $E°(XH^{+\bullet}/XH)$ calculated by CBS-QB3 and B3LYP in water are in very good agreement with each other (MAE = 0.04 V) and

dx.doi.org/10.1021/ct300550x | J. Chem. Theory Comput. 2012, 8, 5107–5123

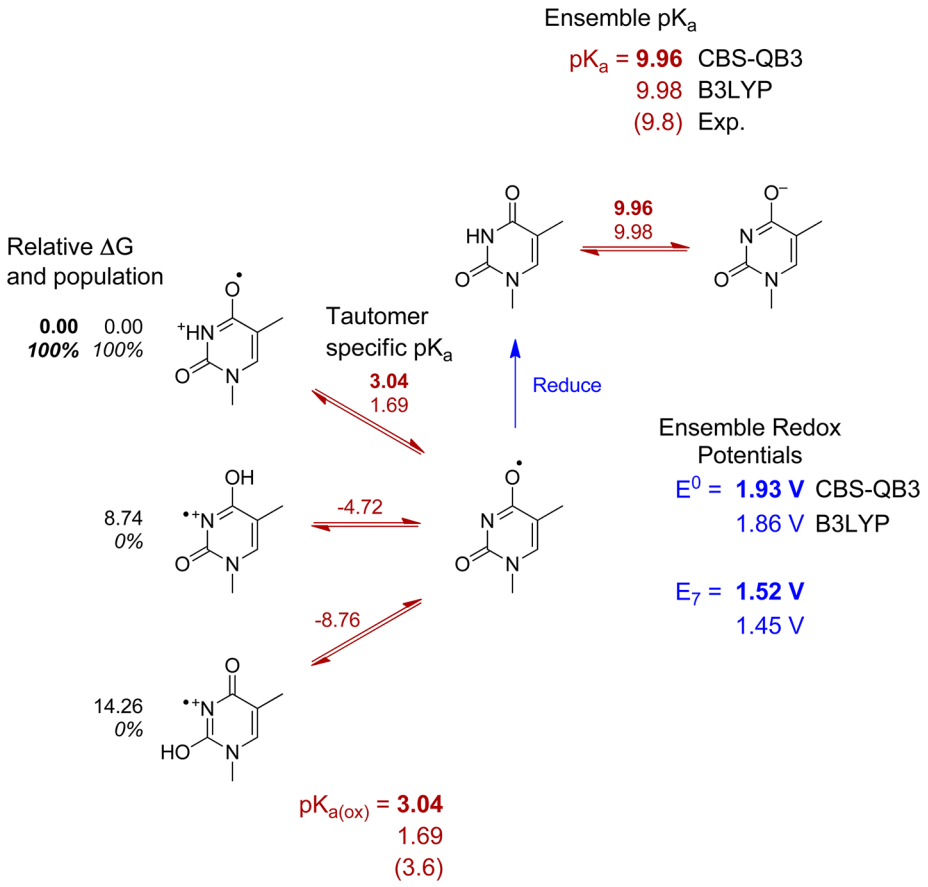

Figure 6. Calculated pK_a's and oxidation potentials for 1-methylthymine. See Figure 3 caption for details.

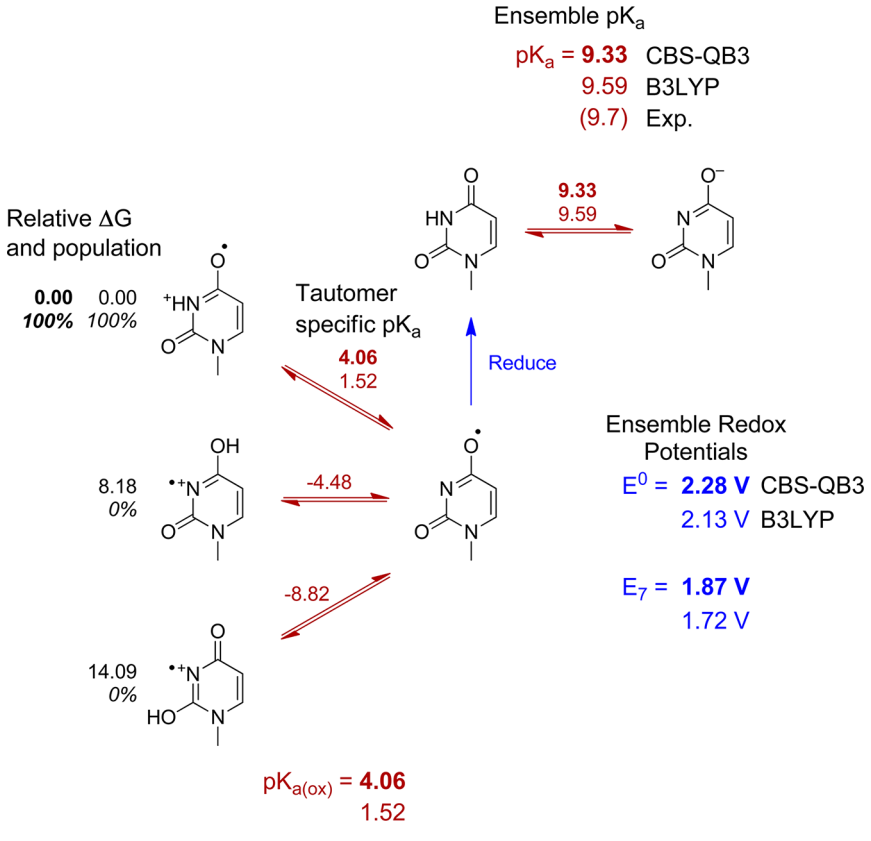

Figure 7. Calculated pK_a's and oxidation potentials for 1-methyluracil. See Figure 3 caption for details.

dx.doi.org/10.1021/ct300550x | J. Chem. Theory Comput. 2012, 8, 5107−5123

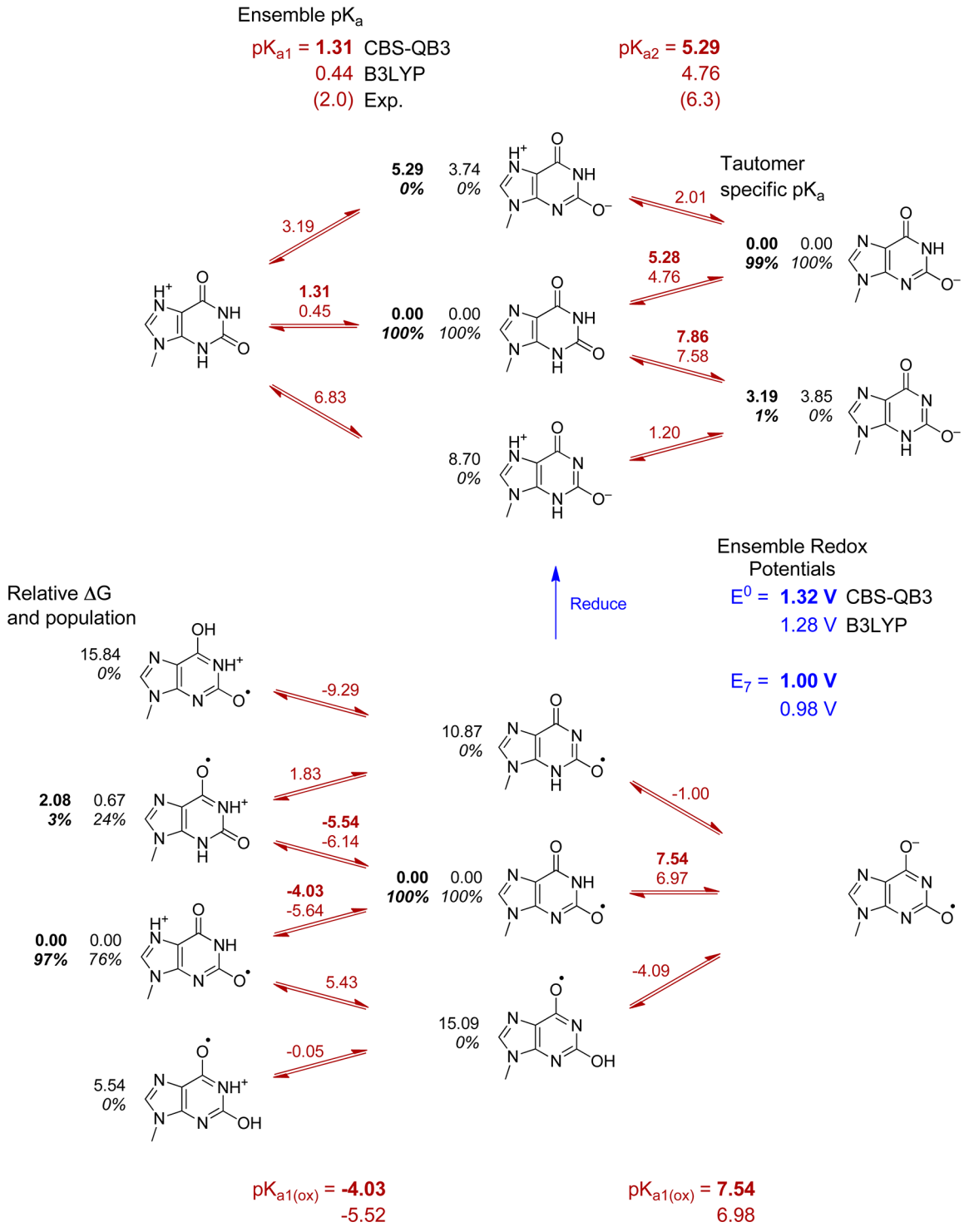

Figure 8. Calculated pK_a's and oxidation potentials for 9-methylxanthine. See Figure 3 caption for details.

compare well with the corresponding calculated values in acetonitrile (0.14 and 0.11 V, respectively).

The present calculations as well as other calculations from the literature agree that $E°(XH^{+\bullet}/XH)$ in water for guanine is 0.3−0.4 V lower than for adenine. Likewise, $E°(XH^{+\bullet}/XH)$ for 8-oxoguanine is calculated to be ca. 0.62 V lower than adenine or ca. 0.3 V lower than guanine. The calculated relative redox potentials in water are 0.01−0.12 V higher than in acetonitrile. Most of the contributions from the solvation energies should cancel when relative redox potentials are compared. The remaining difference can be traced to changes in the radius used for oxygen in SMD; 2.168 Å is used in acetonitrile versus 1.52 Å in water, while the same radii are used for all other atoms. Adenine has no oxygen atoms, whereas the other nucleobases in the table have one or two oxygen atoms, thus affecting the differences in solvation energies between acetonitrile and water. For example, the calculated $E°(XH^{+\bullet}/XH)$ potential for guanine in water using the default oxygen radius of 1.52 Å is 1.20 V. By using an oxygen radius of 2.168 Å in water, the calculated $E°(XH^{+\bullet}/XH)$ potential for guanine is 1.13 V, thus matching

dx.doi.org/10.1021/ct300550x | J. Chem. Theory Comput. 2012, 8, 5107−5123

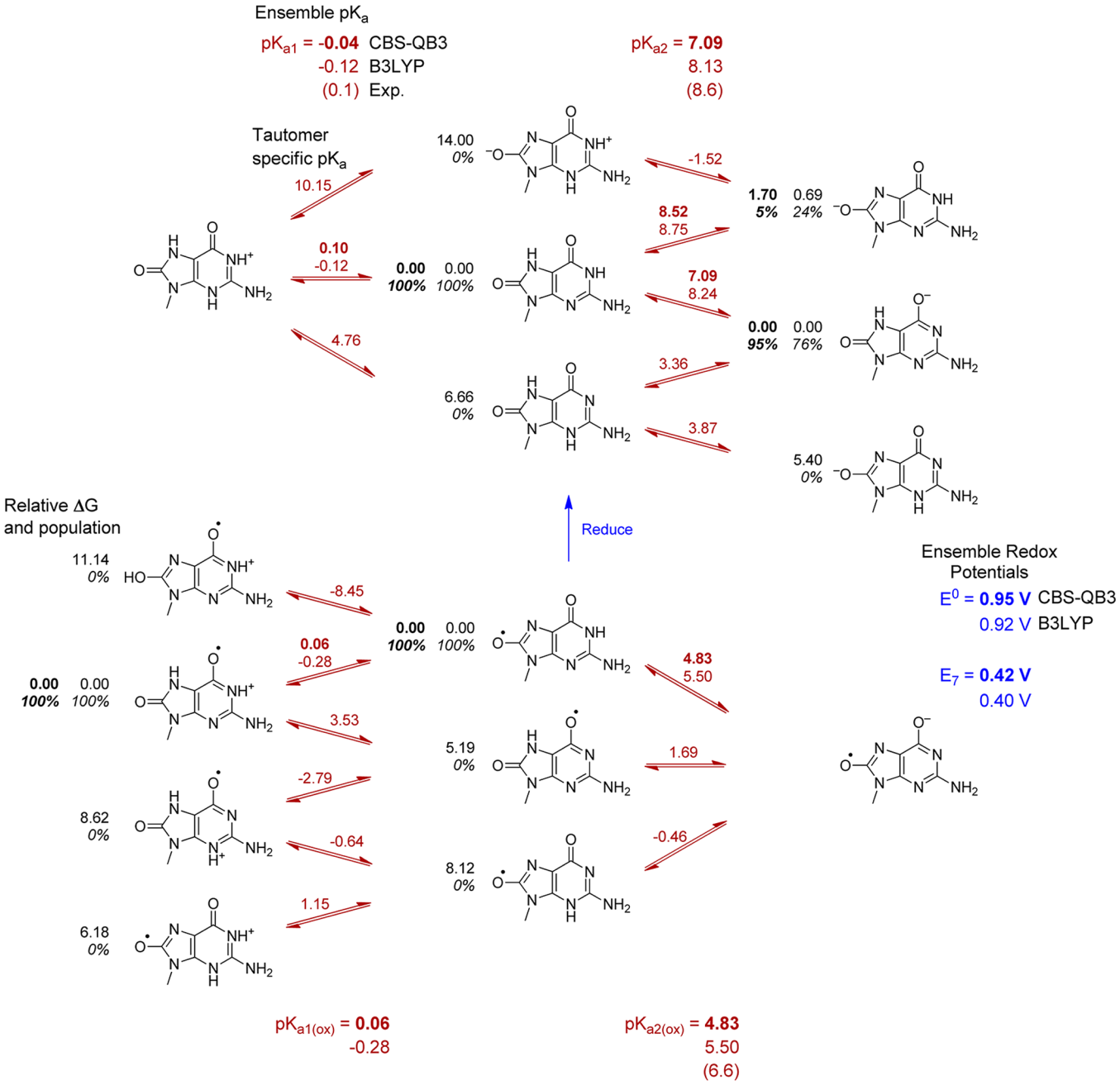

Figure 9. Calculated pK_a's and oxidation potentials for 9-methyl-8-oxoguanine. See Figure 3 caption for details.

the calculated $E°(XH^{+\bullet}/XH)$ potential for guanine in acetonitrile despite the difference in other solvation parameters.

Table 6 lists $E_7(X^{\bullet},H^+/XH)$ for the nucleobases in water. From the pK_a values in Table 3, it is apparent that guanine, adenine, cytosine, thymine, and uracil exist primarily as neutral species at pH 7. Similarly, the oxidized forms of these bases are also neutral at pH 7. Hence, removal of an electron at pH 7 is accompanied by the loss of a proton. Implicit solvation models are generally more accurate for neutral molecules than for ions.[24] In principle, solvent effects should be smaller for $E_7(X^{\bullet},H^+/XH)$ than for $E°(XH^{+\bullet}/XH)$.

Numerous measurements are available for guanosine in aqueous solution. The most widely quoted value is E_7 = 1.29 V versus SHE obtained by Steenken and Jovanovic from kinetic rate measurements.[9] Langmaier et al. obtained E_7 = 1.16 V for guanosine and 1.18 V for 2′-deoxyguanosine from equilibria with $Ru(bpy)_3^{3+/2+}$.[73] Faraggi et al. reported E_7 = 1.17 V for deoxyguanosine by cyclic voltammetry.[10] Several measurements are also available for guanosine monophosphate (GMP). Oliveira-Brett et al. reported E_p for nucleotides by differential pulsed voltammetry; however, the peak values for these irreversible oxidations would have to be corrected for scan rates etc. to estimate E_7.[7] Fukuzumi et al. determined E_7 = 1.31 V for GMP from the kinetics of thermal and photoinduced electron transfer.[74] Faraggi et al. obtained E_7 = 1.25 V for GMP by cyclic voltammetry.[10] Weatherly et al. measured an E_7 potential of 1.28 V for 2′-deoxyguanosine-5′-triphosphate (GTP).[75] The values measured by Langmaier et al. and Xie et al. for GMP were the same as for guanosine.[73,76] These three groups[10,73,76] also obtained E_7's for guanine that were 0.13,

dx.doi.org/10.1021/ct300550x | J. Chem. Theory Comput. 2012, 8, 5107−5123

Table 4. Experimental and Calculated $E°(XH^{+\bullet}/XH)$ Reduction Potentials in Acetonitrile Solution in Volts (V)[a]

	experiment[b]	CBS-QB3[c]	B3LYP[d]	B3LYP[e]
	deoxyribose subst.	methyl subst.	methyl subst.	ribose subst.
	reduction potential versus SCE			
guanine	1.25	1.14	0.96	1.04
adenine	1.72	1.58	1.44	1.41
cytosine	1.90	1.58	1.50	1.57
thymine	1.87	1.63	1.51	1.60
uracil	>2.15	1.91	1.81	1.88
xanthine		1.56	1.41	1.48
8-oxoguanine		0.80	0.64	0.68
MAE to exptl.		*0.21*	*0.33*	*0.28*
	reduction potential relative to adenine			
guanine	−0.47	−0.44	−0.48	−0.37
adenine	0.00	0.00	0.00	0.00
cytosine	0.18	0.01	0.05	0.16
thymine	0.15	0.05	0.07	0.19
uracil	0.43	0.34	0.38	0.47
xanthine		−0.02	−0.04	0.07
8-oxoguanine		−0.77	−0.80	−0.73
MAE to exptl.		*0.10*	*0.07*	*0.05*

[a]Potentials are reported against the absolute potential of SCE in acetonitrile solution (4.429 V).[20] [b]Seidel et al. study determined potentials for DNA nucleosides by cyclic voltammetry in acetonitrile solution.[13] [c]Present study calculated values were obtained for N-methyl substituted bases using an unscaled solvent cavity and CBS-QB3 gas phase free energies. [d]Present study calculated values were obtained for N-methyl substituted bases using an unscaled solvent cavity and B3LYP gas phase free energies. [e]Present study calculated values were obtained for nucleosides using an unscaled solvent cavity and B3LYP gas phase free energies.

Table 5. Aqueous Solution Calculated $E°(XH^{+\bullet}/XH)$ Potential Relative to Adenine in Volts (V)

	present study			
	CBS-QB3	B3LYP		
	methyl subst.	methyl subst.	ribose subst.	unsubst.
guanine	−0.36	−0.39	−0.29	−0.37
adenine	0.00	0.00	0.00	0.00
cytosine	0.11	0.23	0.22	0.32
thymine	0.18	0.19	0.28	0.27
uracil	0.47	0.49	0.53	0.57
xanthine	0.02	0.04	0.16	
8-oxoguanine	−0.62	−0.63	−0.62	
	other computational studies			
	PW91[a]	PMP2[b]	M06-2X[c]	
	unsubst.	unsubst.	unsubst.	
guanine	−0.34	−0.39	−0.37	
adenine	0.00	0.00	0.00	
cytosine	0.44	0.10	0.33	
thymine	0.47	0.24	0.23	
uracil		0.46		
xanthine				
8-oxoguanine	−0.63			

[a]Baik et al.[59] calculated potentials of nucleobases using PW91 level of theory with the COSMO solvation model. [b]Crespo-Hernandez et al.[60] calculated potentials of nucleobases using the PMP2/6-31++G(d,p) level of theory with the PCM solvation model. Molecules were optimized in the gas phase only. [c]Paukku and Hill[91] calculated potentials of nucleobases using the M06−2X/6-31++G(d,p) level of theory with the PCM solvation model.

0.15, and 0.21 V lower than guanosine. In summary, the reported measurements support E_7 = 1.2−1.3 V for guanosine and guanosine monophosphate, with guanine ca. 0.16 V lower. Fewer measurements are available for adenine. A value of 1.42 V was obtained by Steenken et al. for adenosine[9] and by Fukuzumi for the monophosphate,[74] while Faraggi reported 1.32 V for adenine.[10] More experimental data are needed for the oxidation potentials of the pyrimidine nucleobases in water, but thymine appears to be the most readily oxidized of these bases.

The E_7 redox potentials of the methyl substituted bases calculated with CBS-QB3 and B3LYP are in good agreement with each other (MAE = 0.04 V) but have significantly larger differences with experimental values. Compared to the values measured by Steenken et al.[9] for the nucleosides, the MAEs for the calculated redox potentials in water for the methyl substituted bases (0.19 and 0.21 V for CBS-QB3 and B3LYP, respectively) are like those obtained in acetonitrile. Comparable agreement is found with the results of Fukuzumi et al. and Faraggi et al. (MAE = 0.19 V). Li et al. calculated $E_7(X^{\bullet},H^+/XH)$ for unsubstituted bases at the B3LYP/6-311++G(2df,2p) level with COSMO-RS solvation and obtained similar agreement with the experimental values listed in Table 6 (MAE = 0.16 V).[77]

The relative redox potentials should be less sensitive to the solvent and the substituents. Potentials relative to adenine are shown in the bottom half of Table 6. The redox potential of guanine is lower than adenine, but the calculated difference is significantly larger than experimental results. Since the calculated differences in the ionization potentials (Table 2) and the differences in $E°(XH^{+\cdot}/XH)$ in acetonitrile (Table 4) are in good agreement with experimental results, part of the discrepancy must arise from solvent effects in water. As noted above, the SMD model uses different radii for oxygen in acetonitrile and water to try to treat specific solvent interactions. Since guanine has a carbonyl oxygen and adenine does not, this may account for some of the difference in relative redox potentials. Replacing the N9 methyl substituent with ribose decreases the difference by 0.1 V at the B3LYP level. Langmaier found a decrease of 0.23 V at the RIMP2/cc-pVDZ level and traced it to opposing changes in the ionization potential and the proton affinity on going from guanine to guanosine.[73] This brings the calculated difference in the guanosine and adenosine redox potentials in better agreement with experimental results. The calculated redox potential of xanthine is in good agreement with the results of Faraggi et al.[10] The computed values for 8-oxoguanine are too low, but the calculated difference between guanine and 8-oxoguanine (0.53−0.56 V) is in good agreement with the measurements of Steenken et al. (0.55 V).[8]

In agreement with measured values for the pyrimidine bases, calculations with the SMD solvation model indicate that redox potentials of cytosine and thymine are similar in acetonitrile, but thymine is oxidized more easily than cytosine in water at pH 7. The calculations also indicate that the redox potential of uracil is ca. 0.3 V higher than thymine in acetonitrile and in water. The experimental difference is 0.29 V in acetonitrile but only 0.05 V in water. While the calculated redox potentials of cytosine, thymine, and uracil relative to adenine are in good agreement with experimental results in acetonitrile, they are

dx.doi.org/10.1021/ct300550x | J. Chem. Theory Comput. 2012, 8, 5107−5123

Table 6. Experimental and Calculated E_7 Reduction Potentials in Aqueous Solution in Volts (V)[a]

	exptl.			present study			Li et al.
	Steenken et al.[b] ribose subst.	Fukuzumi et al.[c] deoxyribose nucleotide	Faraggi et al.[d] unsubst.	CBS-QB3[f] methyl subst.	B3LYP[f] methyl subst.	B3LYP[g] ribose subst.	B3LYP[h] unsubst.
			reduction potential versus SHE				
guanine	1.29	1.31	1.04[e]	0.95	0.96	1.03	1.06
adenine	1.42	1.42	1.32	1.35	1.38	1.35	1.34
cytosine	~1.6	1.50	1.44[e]	1.66	1.67	1.77	1.72
thymine	~1.7	1.45	1.29	1.52	1.45	1.61	1.38
uracil			1.34[e]	1.87	1.72	1.78	1.58
xanthine			0.93	1.00	0.98		
8-oxoguanine	0.74			0.42	0.40	0.50	0.83
			reduction potential relative to adenine				
guanine	−0.13	−0.11	−0.28	−0.40	−0.42	−0.32	−0.28
adenine	0.00	0.00	0.00	0.00	0.00	0.00	0.00
cytosine	~0.18	0.19	0.12	0.31	0.29	0.42	0.38
thymine	~0.28	0.14	−0.03	0.17	0.07	0.26	0.04
uracil			0.02	0.51	0.34	0.43	0.24
xanthine			−0.39	−0.35	−0.40		
8-oxoguanine	−0.68			−0.93	−0.98	−0.85	−0.51

[a]Potentials are reported against the absolute potential of SHE in aqueous solution (4.281 V). [b]Steenken et al. measured nucleoside potentials using kinetic rate measurement in aqueous solution.[8,9] [c]Fukuzumi et al. measured DNA nucleotide potentials by cyclic voltammetry in aqueous solution.[74] [d]Faraggi et al. measured nucleobase potentials by cyclic voltammetry in aqueous solution.[10] [e]Values are estimated based on an extrapolation of 0.06 V per pH from measured potentials at higher pH.[10] [f]Calculated for N-methylated nucleobases from the corresponding computed values for $E°$ and pK_a using eq 16. [g]Calculated for nucleosides from the corresponding computed $E°$ corrected by the hydrogen ion concentration, $\log[H^+]$. [h]Li et al. calculated values for nonmethylated nucleobases at the B3LYP/6-311++G(2df,2p)/B3LYP//6-31+G(d) level of theory.[77] Potentials are reported against an absolute SHE potential of 4.43 V.

0.1−0.5 V too high in water. This suggests that it may be necessary to go beyond the SMD model to treat specific solvent interactions that occur in water. Alternatively, inconsistencies among the few measured values that are available for these bases suggest that new experimental studies may be needed to clarify the situation.

SUMMARY

Using an appropriate thermodynamic cycle, pK_a's and redox potentials can be calculated from gas phase basicities, adiabatic ionization potentials, and solvation energies. Equilibria between various tautomers must be taken into account when determining the pK_a's. In turn, the pK_a's for the neutral and oxidized nucleobases are needed in the calculation of redox potentials at a given pH. With suitable choices of model chemistries, gas phase basicities and ionization potentials can be calculated to near chemical accuracy (MAE of 1 kcal/mol or 0.05 eV). However, implicit solvation models have greater uncertainties, especially for ions and protic solvents. The scaling of solvent cavities improves the calculation of solvation energies. After scaling, the calculated MAEs for the pK_a's of the nucleobases are 0.7 for B3LYP and 0.9 for CBS-QB3. Nevertheless, there is still some uncertainty in the calculated and experimental pK_a's for a number of the oxidized nucleobases. The calculated redox potentials in acetonitrile are lower than experimental results by 0.18 V for CBS-QB3 and 0.30 for B3LYP, indicating that there is still a systematic error (in part, because of the implicit solvation model). Much of this systematic error cancels if relative redox potentials are compared to experimental results (MAE = 0.10 V for CBS-QB3 and 0.07 V for B3LYP for redox potentials in acetonitrile relative to adenine). For redox potentials in water, solubility problems, irreversible chemical reactions involving labile radical species, and somewhat conflicting measurements complicate the interpretation of the experimental data. Because of problems with irreversibility in electrochemical measurements of the nucleobases in water, redox potentials obtained from equilibria or kinetics measurements appear to be more reliable. For guanosine and guanosine monophosphate, E_7 = 1.2−1.3 V, while guanine is ca. 0.16 V lower. Adenosine and its monophosphate have E_7 = 1.42 V. Of the remaining standard bases, thymine seems to be the most readily oxidized in water, but there is no consensus on the measured oxidation potentials of the pyrimidine bases. The B3LYP and CBS-QB3 calculations have MAEs of 0.21 and 0.19 V for $E_7(X^{\bullet},H^+/XH)$. The larger MAEs reflect the difficulty in treating solvation effects in water with implicit models and also the greater uncertainty in the experimental values. The calculated difference between the guanine and 8-oxoguanine oxidation potentials is in good agreement with experimental values, but the calculated difference between guanine and adenine is too large. Replacing the methyl substituent with ribose changes the calculated E_7 potentials by 0.1−0.2 V. The fact that the MAEs for redox potentials in water are significantly larger than the MAEs in acetonitrile suggests that a better solvation model may be needed for water, perhaps including explicit solvent molecules. On the other hand, new measurements of the redox potentials for nucleobases, methylated nucleobases, and nucleosides in water using identical experimental conditions would help resolve some of the experimental data differences.

ASSOCIATED CONTENT

Supporting Information

A text file containing Cartesian coordinates for all optimized species, a spreadsheet containing all relevant energetic data needed for reproducing reported values in the table and text, and a table containing ionization and oxidation potentials for

reference compound species. This information is available free of charge via the Internet at http://pubs.acs.org

AUTHOR INFORMATION

Corresponding Author

*E-mail: hbs@chem.wayne.edu.

Notes

The authors declare no competing financial interest.

ACKNOWLEDGMENTS

This work was supported by a grant from the National Science Foundation (CHE0910858 and CHE1212281). Wayne State University's computing grid provided computational support.

REFERENCES

(1) Pratviel, G.; Meunier, B. *Chem.—Eur. J.* **2006**, *12*, 6018−6030.
(2) Gimisis, T.; Cismas, C. *Eur. J. Org. Chem.* **2006**, 1351−1378.
(3) Burrows, C. J.; Muller, J. G. *Chem. Rev.* **1998**, *98*, 1109−1151.
(4) Cadet, J.; Berger, M.; Douki, T.; Morin, B.; Raoul, S.; Ravanat, J. L.; Spinelli, S. *Biol. Chem.* **1997**, *378*, 1275−1286.
(5) Breen, A. P.; Murphy, J. A. *Free Radical Biol. Med.* **1995**, *18*, 1033−1077.
(6) Ames, B. N.; Shigenaga, M. K.; Hagen, T. M. *Proc. Natl. Acad. Sci. U. S. A.* **1993**, *90*, 7915−7922.
(7) Oliveira-Brett, A. M.; Piedade, J. A. P.; Silva, L. A.; Diculescu, V. C. *Anal. Biochem.* **2004**, *332*, 321−329.
(8) Steenken, S.; Jovanovic, S. V.; Bietti, M.; Bernhard, K. *J. Am. Chem. Soc.* **2000**, *122*, 2373−2374.
(9) Steenken, S.; Jovanovic, S. V. *J. Am. Chem. Soc.* **1997**, *119*, 617−618.
(10) Faraggi, M.; Broitman, F.; Trent, J. B.; Klapper, M. H. *J. Phys. Chem.* **1996**, *100*, 14751−14761.
(11) Steenken, S. *Chem. Rev.* **1989**, *89*, 503−520.
(12) Jovanovic, S. V.; Simic, M. G. *J. Phys. Chem.* **1986**, *90*, 974−978.
(13) Seidel, C. A. M.; Schulz, A.; Sauer, M. H. M. *J. Phys. Chem.* **1996**, *100*, 5541−5553.
(14) Sviatenko, L.; Isayev, O.; Gorb, L.; Hill, F.; Leszczynski, J. *J. Comput. Chem.* **2011**, *32*, 2195−2203.
(15) Namazian, M.; Lin, C. Y.; Coote, M. L. *J. Chem. Theory Comput.* **2010**, *6*, 2721−2725.
(16) Lewis, A.; Bumpus, J. A.; Truhlar, D. G.; Cramer, C. J. *J. Chem. Educ.* **2004**, *81*, 596−604.
(17) Lewis, A.; Bumpus, J. A.; Truhlar, D. G.; Cramer, C. J. *J. Chem. Educ.* **2007**, *84*, 934−934.
(18) Ho, J. M.; Coote, M. L. *Theor. Chem. Acc.* **2010**, *125*, 3−21.
(19) Ho, J. M.; Coote, M. L. *Wiley Interdiscip. Rev.: Comput. Mol. Sci.* **2011**, *1*, 649−660.
(20) Isse, A. A.; Gennaro, A. *J. Phys. Chem. B* **2010**, *114*, 7894−7899.
(21) Kelly, C. P.; Cramer, C. J.; Truhlar, D. G. *J. Phys. Chem. B* **2006**, *110*, 16066−16081.
(22) Camaioni, D. M.; Schwerdtfeger, C. A. *J. Phys. Chem. A* **2005**, *109*, 10795−10797.
(23) Roy, L. E.; Jakubikova, E.; Guthrie, M. G.; Batista, E. R. *J. Phys. Chem. A* **2009**, *113*, 6745−6750.
(24) Marenich, A. V.; Cramer, C. J.; Truhlar, D. G. *J. Phys. Chem. B* **2009**, *113*, 6378−6396.
(25) Ben-Naim, A.; Marcus, Y. *J. Chem. Phys.* **1984**, *81*, 2016−2027.
(26) Stephens, P. J.; Devlin, F. J.; Chabalowski, C. F.; Frisch, M. J. *J. Phys. Chem.* **1994**, *98*, 11623−11627.
(27) Becke, A. D. *J. Chem. Phys.* **1993**, *98*, 5648−5652.
(28) Lee, C. T.; Yang, W. T.; Parr, R. G. *Phys. Rev. B* **1988**, *37*, 785−789.
(29) Becke, A. D. *Phys. Rev. A* **1988**, *38*, 3098−3100.
(30) Vosko, S. H.; Wilk, L.; Nusair, M. *Can. J. Phys.* **1980**, *58*, 1200−1211.
(31) Francl, M. M.; Pietro, W. J.; Hehre, W. J.; Binkley, J. S.; Gordon, M. S.; Defrees, D. J.; Pople, J. A. *J. Chem. Phys.* **1982**, *77*, 3654−3665.
(32) Gordon, M. S. *Chem. Phys. Lett.* **1980**, *76*, 163−168.
(33) Hariharan, P. C.; Pople, J. A. *Mol. Phys.* **1974**, *27*, 209−214.
(34) Hariharan, P. C.; Pople, J. A. *Theor. Chim. Acta* **1973**, *28*, 213−222.
(35) Hehre, W. J.; Ditchfield, R.; Pople, J. A. *J. Chem. Phys.* **1972**, *56*, 2257.
(36) Ditchfield, R.; Hehre, W. J.; Pople, J. A. *J. Chem. Phys.* **1971**, *54*, 724−728.
(37) Kendall, R. A.; Dunning, T. H.; Harrison, R. J. *J. Chem. Phys.* **1992**, *96*, 6796−6806.
(38) Montgomery, J. A.; Frisch, M. J.; Ochterski, J. W.; Petersson, G. A. *J. Chem. Phys.* **2000**, *112*, 6532−6542.
(39) Montgomery, J. A.; Frisch, M. J.; Ochterski, J. W.; Petersson, G. A. *J. Chem. Phys.* **1999**, *110*, 2822−2827.
(40) Frisch, M. J.; Trucks, G. W.; Schlegel, H. B.; Scuseria, G. E.; Robb, M. A.; et al. *Gaussian Development Version*, GDVRev. H20+; Gaussian, Inc.: Wallingford, CT, 2010.
(41) Scalmani, G.; Frisch, M. J. *J. Chem. Phys.* **2010**, *132*, 114110.
(42) Cossi, M.; Barone, V.; Mennucci, B.; Tomasi, J. *Chem. Phys. Lett.* **1998**, *286*, 253−260.
(43) Mennucci, B.; Tomasi, J. *J. Chem. Phys.* **1997**, *106*, 5151−5158.
(44) Cances, E.; Mennucci, B.; Tomasi, J. *J. Chem. Phys.* **1997**, *107*, 3032−3041.
(45) Munk, B. H.; Burrows, C. J.; Schlegel, H. B. *Chem. Res. Toxicol.* **2007**, *20*, 432−444.
(46) Wardman, P. *J. Phys. Chem. Ref. Data* **1989**, *18*, 1637−1755.
(47) Clark, W. M. *Oxidation-Reduction Potentials of Organic Systems*; Williams & Wilkins: Baltimore, MD, 1960; pp 107−148.
(48) Dawson, R. M. C. *Data for Biochemical Research*, 3rd ed.; Clarendon Press: Oxford, U. K., 1986; pp 103−114.
(49) Verdolino, V.; Cammi, R.; Munk, B. H.; Schlegel, H. B. *J. Phys. Chem. B* **2008**, *112*, 16860−16873.
(50) Jang, Y. H.; Goddard, W. A.; Noyes, K. T.; Sowers, L. C.; Hwang, S.; Chung, D. S. *J. Phys. Chem. B* **2003**, *107*, 344−357.
(51) Jang, Y. H.; Goddard, W. A.; Noyes, K. T.; Sowers, L. C.; Hwang, S.; Chung, D. S. *Chem. Res. Toxicol.* **2002**, *15*, 1023−1035.
(52) Bartmess, J. E. *J. Phys. Chem.* **1994**, *98*, 6420−6424.
(53) Bartmess, J. E. *J. Phys. Chem.* **1995**, *99*, 6755−6755.
(54) Moser, A.; Range, K.; York, D. M. *J. Phys. Chem. B* **2010**, *114*, 13911−13921.
(55) Baboul, A. G.; Curtiss, L. A.; Redfern, P. C.; Raghavachari, K. *J. Chem. Phys.* **1999**, *110*, 7650−7657.
(56) Liu, M.; Li, T. T.; Amegayibor, F. S.; Cardoso, D. S.; Fu, Y. L.; Lee, J. K. *J. Org. Chem.* **2008**, *73*, 9283−9291.
(57) Wolken, J. K.; Turecek, F. *J. Am. Soc. Mass Spectrom.* **2000**, *11*, 1065−1071.
(58) Close, D. M. *J. Phys. Chem. A* **2004**, *108*, 10376−10379.
(59) Baik, M. H.; Silverman, J. S.; Yang, I. V.; Ropp, P. A.; Szalai, V. A.; Yang, W. T.; Thorp, H. H. *J. Phys. Chem. B* **2001**, *105*, 6437−6444.
(60) Crespo-Hernandez, C. E.; Arce, R.; Ishikawa, Y.; Gorb, L.; Leszczynski, J.; Close, D. M. *J. Phys. Chem. A* **2004**, *108*, 6373−6377.
(61) Schlegel, H. B. *J. Chem. Phys.* **1986**, *84*, 4530−4534.
(62) Lin, J.; Yu, C.; Peng, S.; Akiyama, I.; Li, K.; Lee, L. K.; Lebreton, P. R. *J. Phys. Chem.* **1980**, *84*, 1006−1012.
(63) Lin, J.; Yu, C.; Peng, S.; Akiyama, I.; Li, K.; Lee, L. K.; Lebreton, P. R. *J. Am. Chem. Soc.* **1980**, *102*, 4627−4631.
(64) Yu, C.; Peng, S.; Akiyama, I.; Lin, J.; Lebreton, P. R. *J. Am. Chem. Soc.* **1978**, *100*, 2303−2307.
(65) Dougherty, D.; Wittel, K.; Meeks, J.; McGlynn, S. P. *J. Am. Chem. Soc.* **1976**, *98*, 3815−3820.
(66) Denifl, S.; Sonnweber, B.; Hanel, G.; Scheier, P.; Mark, T. D. *Int. J. Mass Spectrom.* **2004**, *238*, 47−53.
(67) Crespo-Hernandez, C. E.; Close, D. M.; Gorb, L.; Leszczynski, J. *J. Phys. Chem. B* **2007**, *111*, 5386−5395.
(68) Ginovska, B.; Camaioni, D. M.; Dupuis, M. *J. Chem. Phys.* **2008**, *129*, 014506.
(69) Caricato, M.; Mennucci, B.; Tomasi, J. *Mol. Phys.* **2006**, *104*, 875−887.

(70) Fu, Y.; Liu, L.; Yu, H. Z.; Wang, Y. M.; Guo, Q. X. *J. Am. Chem. Soc.* **2005**, *127*, 7227−7234.
(71) Orozco, M.; Luque, F. J. *Chem. Phys.* **1994**, *182*, 237−248.
(72) Bachs, M.; Luque, F. J.; Orozco, M. *J. Comput. Chem.* **1994**, *15*, 446−454.
(73) Langmaier, J.; Samec, Z.; Samcova, E.; Hobza, P.; Reha, D. *J. Phys. Chem. B* **2004**, *108*, 15896−15899.
(74) Fukuzumi, S.; Miyao, H.; Ohkubo, K.; Suenobu, T. *J. Phys. Chem. A* **2005**, *109*, 3285−3294.
(75) Weatherly, S. C.; Yang, I. V.; Thorp, H. H. *J. Am. Chem. Soc.* **2001**, *123*, 1236−1237.
(76) Xie, H.; Yang, D. W.; Heller, A.; Gao, Z. Q. *Biophys. J.* **2007**, *92*, L70−L72.
(77) Li, M. J.; Liu, W. X.; Peng, C. R.; Lu, W. C. *Acta Phys.—Chim. Sin.* **2011**, *27*, 595−603.
(78) Hunter, E. P. L.; Lias, S. G. *J. Phys. Chem. Ref. Data* **1998**, *27*, 413−656.
(79) Greco, F.; Liguori, A.; Sindona, G.; Uccella, N. *J. Am. Chem. Soc.* **1990**, *112*, 9092−9096.
(80) Meotner, M. *J. Am. Chem. Soc.* **1979**, *101*, 2396−2403.
(81) Wilson, M. S.; McCloskey, J. A. *J. Am. Chem. Soc.* **1975**, *97*, 3436−3444.
(82) Zhachkina, A.; Liu, M.; Sun, X. J.; Amegayibor, F. S.; Lee, J. K. *J. Org. Chem.* **2009**, *74*, 7429−7440.
(83) Chen, E. C. M.; Herder, C.; Chen, E. S. *J. Mol. Struct.* **2006**, *798*, 126−133.
(84) Orlov, V. M.; Smirnov, A. N.; Varshavsky, Y. M. *Tetrahedron Lett.* **1976**, 4377−4378.
(85) Song, B.; Zhao, J.; Griesser, R.; Meiser, C.; Sigel, H.; Lippert, B. *Chem.—Eur. J.* **1999**, *5*, 2374−2387.
(86) Kampf, G.; Kapinos, L. E.; Griesser, R.; Lippert, B.; Sigel, H. *J. Chem. Soc., Perkin Trans. 2* **2002**, 1320−1327.
(87) Kulikowska, E.; Kierdaszuk, B.; Shugar, D. *Acta Biochim. Pol.* **2004**, *51*, 493−531.
(88) Christensen, J. J.; Rytting, J. H.; Izatt, R. M. *Biochemistry* **1970**, *9*, 4907−4913.
(89) Kobayashi, K. *J. Phys. Chem. B* **2010**, *114*, 5600−5604.
(90) Cho, B. P. *Magn. Reson. Chem.* **1993**, *31*, 1048−1053.
(91) Paukku, Y.; Hill, G. *J. Phys. Chem. A* **2011**, *115*, 6738−6738.